An introduction to Particle Image Velocimetry (PIV)

Principles and Applications

Fabio Cozzi

Laboratorio di Combustione

Dip. di Energia, Politecnico di Milano

April 2014

Imaging Systems

Imaging systems are non intrusive optical techniques for research and diagnostics into flow, turbulence, micro fluidics, spray atomisation and combustion processes.

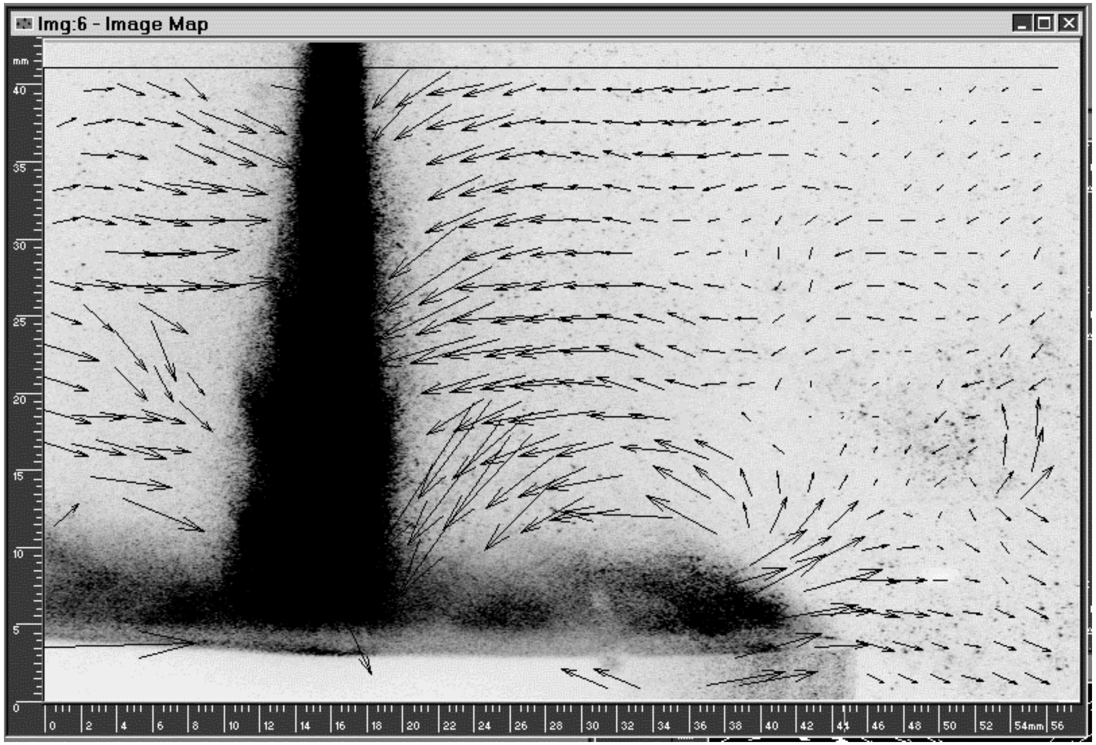

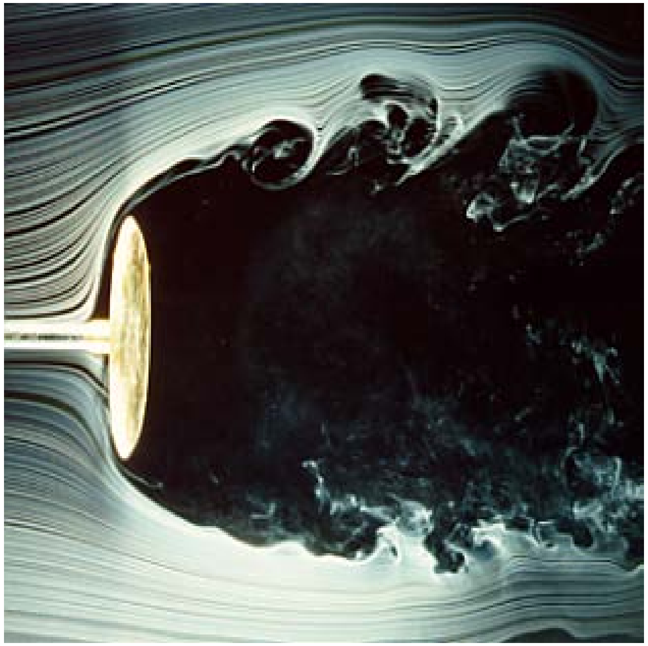

Quantitative Flow Visualization

- Quantitative flow visualization requires the fluid must be seeded with small particle tracers able to follow the instantaneous changes of the flow velocity.
- In order to obtain robust unbiased measurements over the flow domain, it is important that tracer particles are homogeneously distributed within the observed flow region.

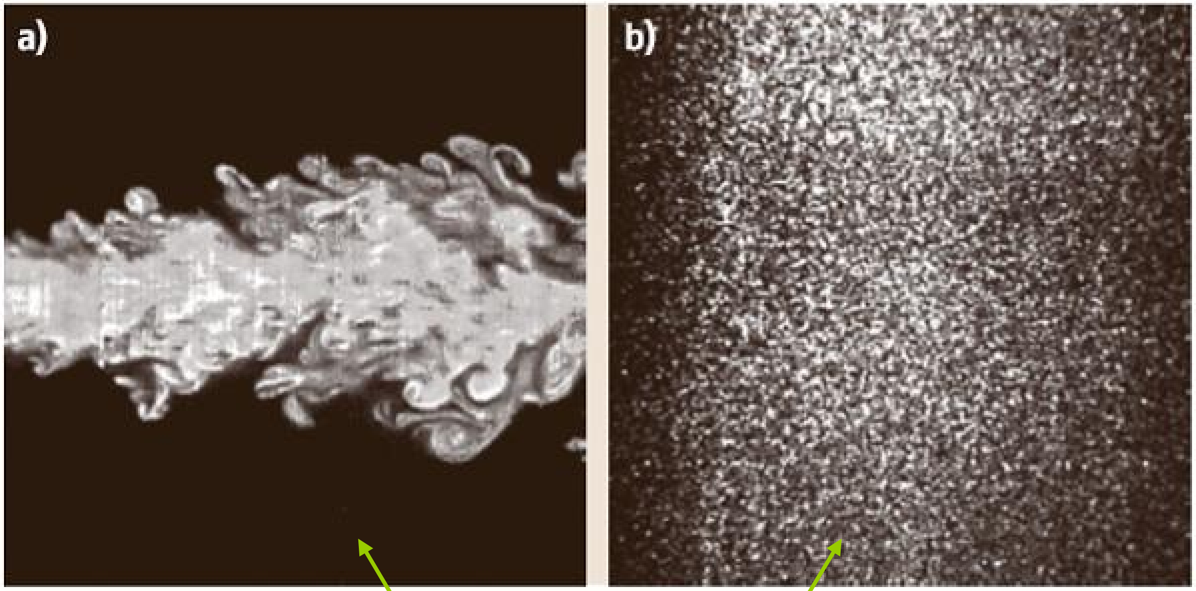

Visualization vs. Measurement

What is PIV?

- PIV stands for ***P****article* ***I****mage* ***V****elocimetry*
- It is a optical diagnostic technique used to measure the velocity field in gas/liquid flows
- Actually the displacement of particles scattered in the flow is measured!

The Principle of PIV

The principle of PIV is based on the measurement of the displacement of small tracer particles that are carried by the fluid during a short time interval.

The tracer particles are sufficiently small that they accurately follow the fluid motion and do not alter the fluid properties or flow characteristics

PIV can be applied to virtually any kind of flow, as long as the fluid is *transparent* and a suitable optical access to the flow is available

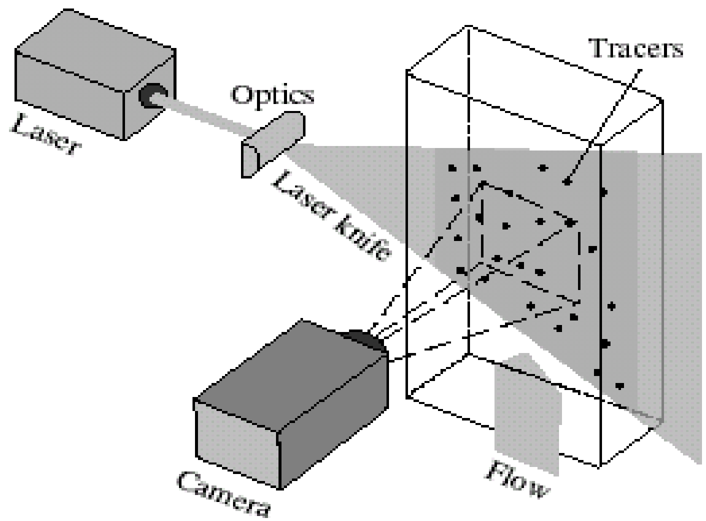

Fig. 1. Schematic of the PIV method.

The Principle of PIV

The basic principle is to take two snapshots of the flowfield at a known time interval, and evaluating the velocity

Once a sequence of two light pulses is recorded, the images are divided into small subsections called interrogation areas (D_I).

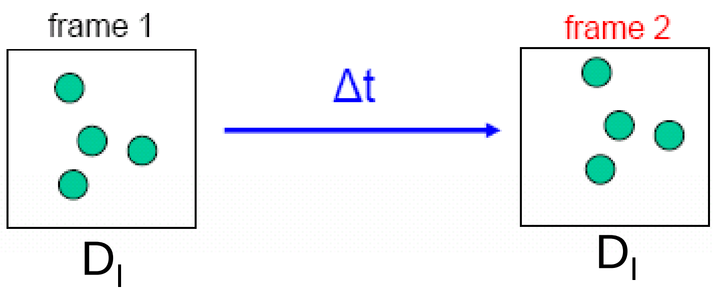

The velocity vectors are statistically derived from each interrogation area by measuring the average displacement of particles between two light pulses:

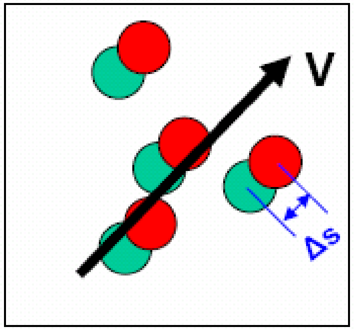

$$\vec{V} = \frac{\Delta \vec{s}}{\Delta t}$$

Why use PIV?

ADVANTAGES

- non-intrusive (besides particles)
- 2 velocity components are readily measured (in a plane!)
- rapid mean flow measurement
- allow flow structures to be visualized
- spatial correlations
- extension to
  - ✓ three velocity components
  - ✓ volume mapping

LIMITATIONS

- needs optical access
- max area of interest about 0.5 m x 0.5 m
- reflections at walls
- safety
- relatively expensive

Components of PIV System

- Light source
  - Laser ....
  - Light sheet formations optics
- Image recording system
  - Camera (film, *CCD*, *CMOS*)
  - Optics (objective + filter)
  - Intensifier (not always needed)
  - Frame grabber (not always needed)
- Synchronization Unit

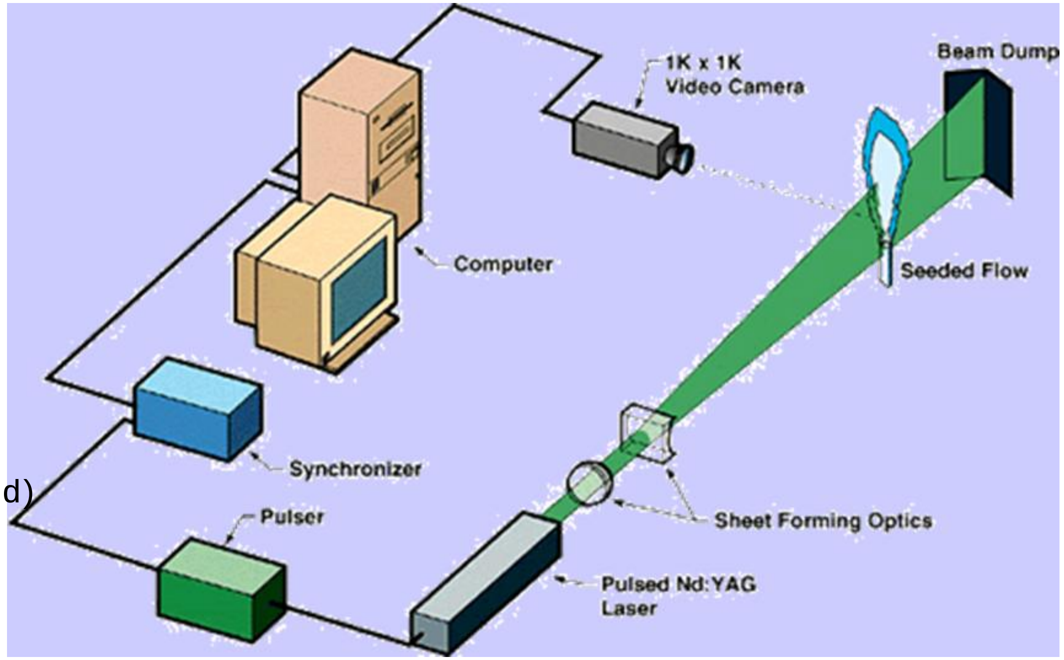

- PIV Image Recording and Processing System
  - PC
  - Storage systems
  - Software
- Seeding system

SEEDING (introduction)

- A very important issue for obtaining accurate PIV measurements is appropriate seeding of the flow with tracer particles.
- To closely follow the flow the particles should be as small as possible, but on the other hand they may not be too small, because then they will not scatter enough light, and hence produce too weak images.
- For liquid flows a particle diameter of d_p = 10-20 μm is a usual compromise.
- In gas flows the particles have to be smaller to follow the flow, because of the lower density of gas compared to liquid. In gas flows a usual compromise of particle size is d_p = 1-5 μm.
- **It is desirable that seeding particles be**
  non-toxic, non-corrosive, non-abrasive, non-volatile and chemically inert.

SEEDING (particle motion in flows)

- At low Reynolds number the motion of a spherical particle is describe by BBO equation

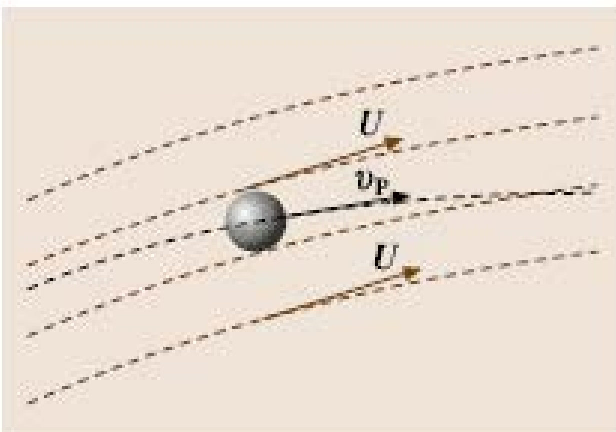

a = particles radius
$\boldsymbol{v_p}$ = particles velocities
$\boldsymbol{U}$ = gas velocities
$\boldsymbol{V} = \boldsymbol{v_p} - \boldsymbol{U}$

$$\frac{4}{3}\pi a^3 \rho_{\mathrm{p}} \frac{\mathrm{d}\boldsymbol{v}}{\mathrm{d}t} = \underbrace{\cancel{\frac{4}{3}\pi a^3 \rho_{\mathrm{f}} \frac{\mathrm{D}\boldsymbol{V}}{\mathrm{D}t}}}_{\text{non-inertial force}} + \underbrace{\cancel{\frac{4}{3}\pi a^3(\rho_{\mathrm{p}} - \rho_{\mathrm{f}})\boldsymbol{g}}}_{\text{net body force}}$$

$$\underbrace{- 6\pi\mu a\left[(\boldsymbol{v}_{\mathrm{p}} - \boldsymbol{U}) - \cancel{\frac{1}{6}a^2\nabla^2\boldsymbol{U}}\right]}_{\text{quasi-steady viscous force}}$$

$$\underbrace{- 6\pi\mu a^2 \int_0^t \frac{\mathrm{d}}{\mathrm{d}\tau}\left[\cancel{(\boldsymbol{v}_{\mathrm{p}} - \boldsymbol{U}) - \frac{1}{6}}a^2\nabla^2\boldsymbol{U}\right]\frac{\mathrm{d}\tau}{\sqrt{\nu(t-\tau)}}}_{\text{time history (Basset) force}}$$

$$\underbrace{- \frac{2}{3}\pi a^3 \frac{\mathrm{d}}{\mathrm{d}t}\left[\cancel{(\boldsymbol{v}_{\mathrm{p}} - \boldsymbol{U}) - \frac{1}{10}}a^2\nabla^2\boldsymbol{U}\right]}_{\text{added mass force}} + \underbrace{\cancel{\boldsymbol{L}}}_{\text{lift force}},$$

Basset–Boussinesq–Oseen (BBO) equation

SEEDING (particle motion in flows)

According to previous approximations a small particle moving in a fluid is described by the equation of motion

$$\frac{4}{3}\pi a^3 \rho_p \frac{dv_p}{dt} = \frac{C_D}{2}\pi a^2 \rho_f V^2 \qquad \mathrm{Re}_p = \frac{2a\rho_f V}{\mu}$$

μ: fluid viscosity, C_D: drag coefficient, V relative gas velocity

In the Stokes regime ($\mathrm{Re}_p < 1$) $C_D = 24/\mathrm{Re}_p$ and if $\rho_p >> \rho_f$

The particle has a characteristic response time: $\tau = \frac{1}{18}\frac{\rho_p d_p^{\,2}}{\mu}$

and assumes the local fluid velocity exponentially.

In swirling flows the seeding particles are forced outwards in a manner that depends critically on the particle diameter, particle mass and vortex circulation. In this case the particle characteristic time should be less than the vortex time scale.

SEEDING (particle motion in flows)

- Example

100 μm oil particle in air ($\rho_p = 900\ kg/m^3$) $\tau \sim 0.03$ s

10 μm oil particle in air ($\rho_p = 900\ kg/m^3$) $\tau \sim 0.0003$ s

10 μm Al_2O_3 particle in water ($\rho_p = 3960\ kg/m^3$) $\tau \sim 0.00003$ s

SEEDING (particle motion in flows)

$\rho_p >> \rho_f$

$$\frac{U_p}{U_f} = \frac{1}{\sqrt{1+\omega^2\tau^2}}$$

$$\tau = \frac{1}{18}\frac{\rho_p d_p{}^2}{\mu}$$

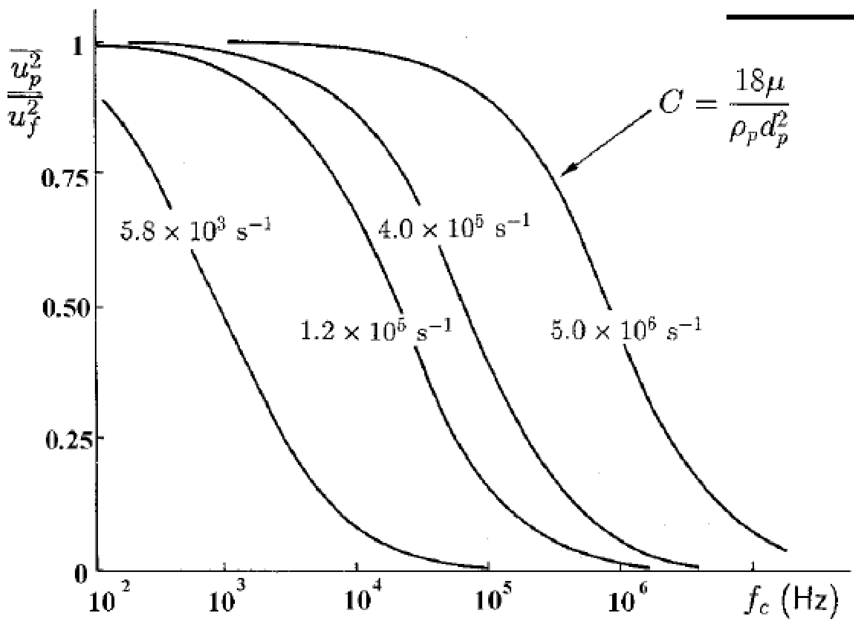

Table 2. Particle response in turbulent flow $(U_p/U_f = 0.99)$

Particle	ρ_p (kg m^{-3})	Gas (10^5 Pa)	Density ratio s	Viscosity ν (m^2 s^{-1})	f_c (kHz)	Sk_c	d_p (μm)
TiO_2	3500	Air (300 K)	2950	1.50×10^{-5}	1	0.0295	1.44
					10		0.45
Al_2O_3	3970	Flame (1800 K)	20250	3.00×10^{-4}	1	0.0113	2.46
					10		0.78
Glass	2600	Air (300 K)	2190	1.50×10^{-5}	1	0.0342	1.67
					10		0.53
Olive oil	970	Air (220 K)	617	1.45×10^{-5}	1	0.0645	3.09
					10		0.98
Microballoon	100	Air (300 K)	84.5	1.50×10^{-5}	1	0.1742	8.50
					10		2.69

$$Sk = \left(\frac{\omega}{\nu}\right)^{1/2} d_p$$

$$\nu = \mu/\rho_f$$

SEEDING

For PIV-LDV applications in isothermal flows the best solution is to filter the air and introduce artificially generated aerosol particles.

The injection of seeding particles can perturb the reacting flow through:

- Catalitic effects
- Heat exchange (cooling of the gas)
- Absorption of light (obscuration)
- Particles/vortices interactions (typically particles are smaller then the smallest turbulence scales)

These effects depend also on the particle number concentration.

Typical probe volume dimension: 10^{-11} m^3

Max. $N_p \approx 10^{11}$ m^{-3} (single scattering, LDV)

Particle concentration determines the average Data Rate and frequency resolution of the turbulent velocity spectra.

SEEDING

- GAS FLOW

Material	particle diameter d_p (μm)	Laser	Pulse energy, pulse time	Light sheet w (mm)	Light sheet t (mm)
TiO_2 (m = 2.6, ρ = 3500 kg m^{-3})	<1	Nd:YAG	10 mJ, 20 ns	15	0.3
TiO_2, ZrO_2	0.7–1	Nd:YAG	110 mJ, 12 ns		
Al_2O_3 (m = 1.76, ρ = 3970 kg m^{-3})	0.3	Nd:YAG	400 mJ		0.2
	3	Nd:YAG	9 mJ, 6 ns		
	0.8	Ruby	20 ns	150	$\simeq$1
Polycrystalline	30	Nd:YAG	135 mJ, 6 ns		
Glass	30	Ruby	30 mJ, 30 ns		
Oil smoke	1	Ruby	5 J		
Corn oil	1–2	Nd:YAG	100 mJ		
Oil	1–2	Nd:YAG	120 mJ		0.4
Olive oil (m = 1.47, ρ = 970 kg m^{-3})	1.06	Nd:YAG	70 mJ, 16 ns	200	0.5

Fluid	Material	Diameter (μm)	Density (kg/m^3)
Air	DEHS	1–3	10^3
–	Glycol–water solution	1–3	10^3
–	Vegetable oil	1–3	10^3
–	TiO_2	0.2–0.5	$1-4\times10^3$

Material	Density (g/cm^{-3})	Index of refraction	Melting point (°C)
NaCl	2.16	1.54	801
Al_2O_3	3.96	1.79	2015
TiO_2	4.26	2.6–2.9	1750
SiC	3.2	2.6	2700
ZrO_2	5.6	2.2	2980

SEEDING

LIQUID FLOW

- The higher density/viscosity of liquids as compared to gases allows to use bigger particles
- Bigger particles require less laser power

Material	particle diameter d_p (μm)	Laser	CW power or energy, time	Light sheet w (mm)	Light sheet t (mm)
TiO_2	3	Nd:YAG			
Al_2O_3	9.5	Ruby	2 J, 30 ns	100	0.8
Conifer pollen (ρ = 1000 kg m^{-3})	50–60	Ar ion	1-2 W		
Polymer (ρ = 1030 kg m^{-3})	30	Ar ion	0.5–5 W		0.5
Phosphorescent polymer	80	Ar ion	5 W		1
Fluorescent	50	Nd:YAG			
	20	Cu vapour	45 W		1
Polystyrene	500				
(ρ = 1050 kg m^{-3})	15	Ruby	25 mJ, 20 ns		
Thermoplastic (ρ = 1020 kg m^{-3})	6	Nd:YAG		50	2
Reflective	60	Ar ion	18 W		
(ρ = 1010 kg m^{-3})	30	Ar ion	12–18 W	200	
Metallic coated	4	Ar ion	2 W		2
	14	Ar ion			1
Microspheres (ρ = 700 kg m^{-3})	$<$30	Ar ion			
H_2 bubbles		Ar ion	1 W		0.3

SEEDING

- Aerosol generation

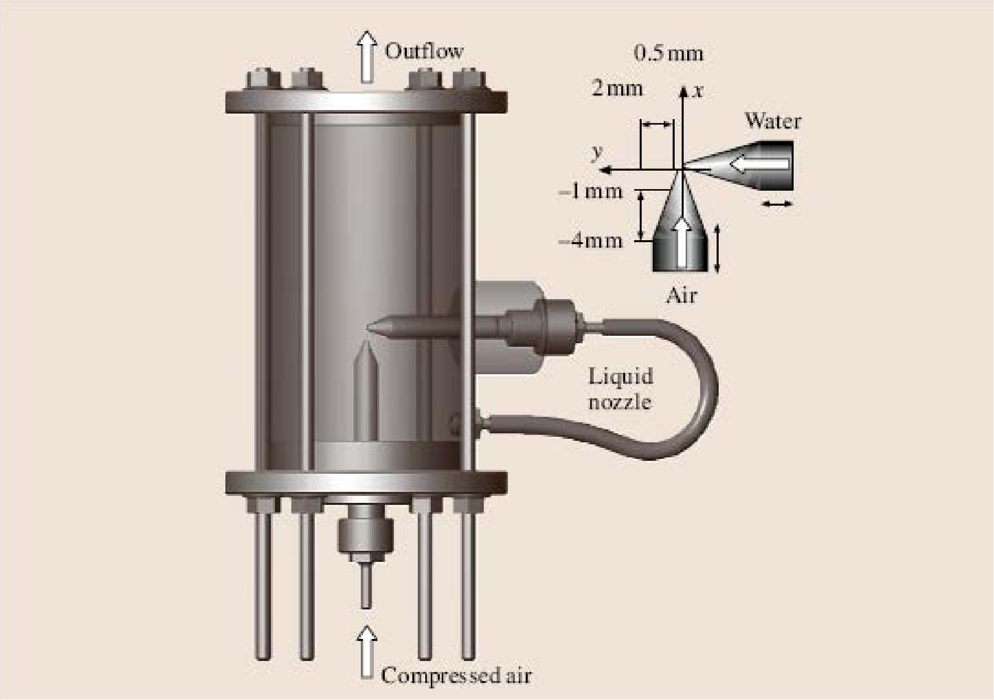

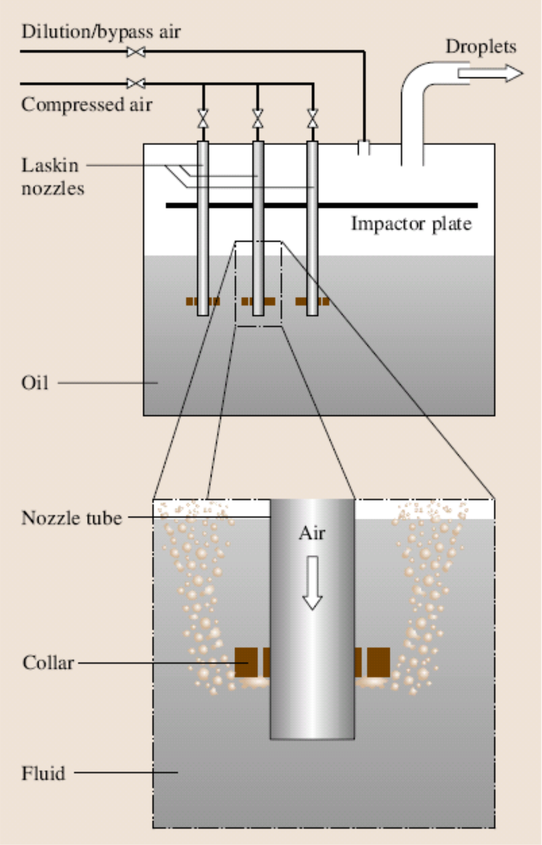

Fig. 5.65 Schematic of a Laskin nozzle unit for droplet seeding

SEEDING

- Aerosol generation

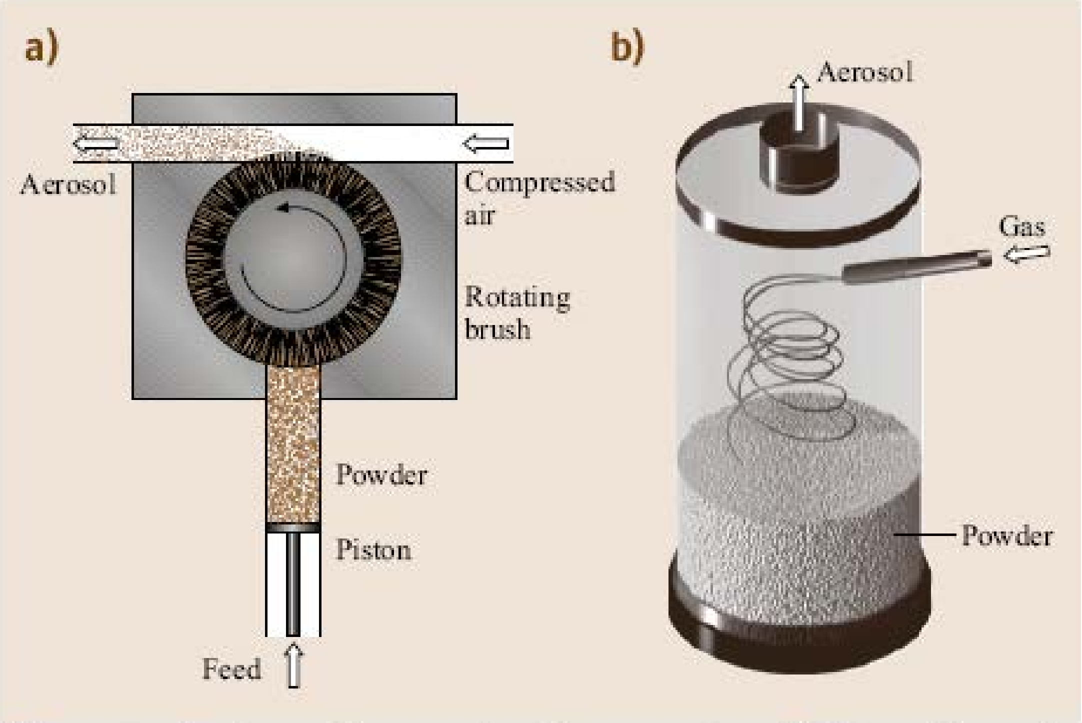

Fig. 5.67a,b Aerosol generation from powder. **(a)** Operation principle of a rotary brush seeder. **(b)** A cyclone aerosol generator

SEEDING (light scattering)

- Laser light is scattered everywhere by the particle
  - The total amount of scattered light, I_0, is a function of:
    Refractive index, light polarization plane, particle diameter, particle shape …..

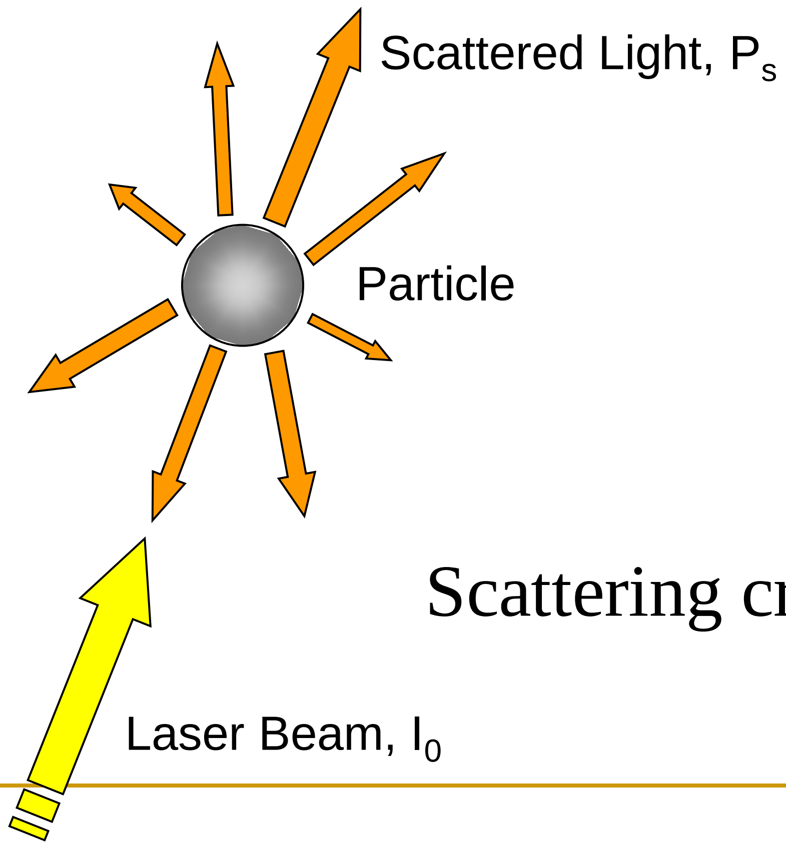

$$\text{Scattering cross section} = P_S / I_0$$

SEEDING (light scattering)

- Computed light scattering cross section as a function of non-dimensional particle diameter

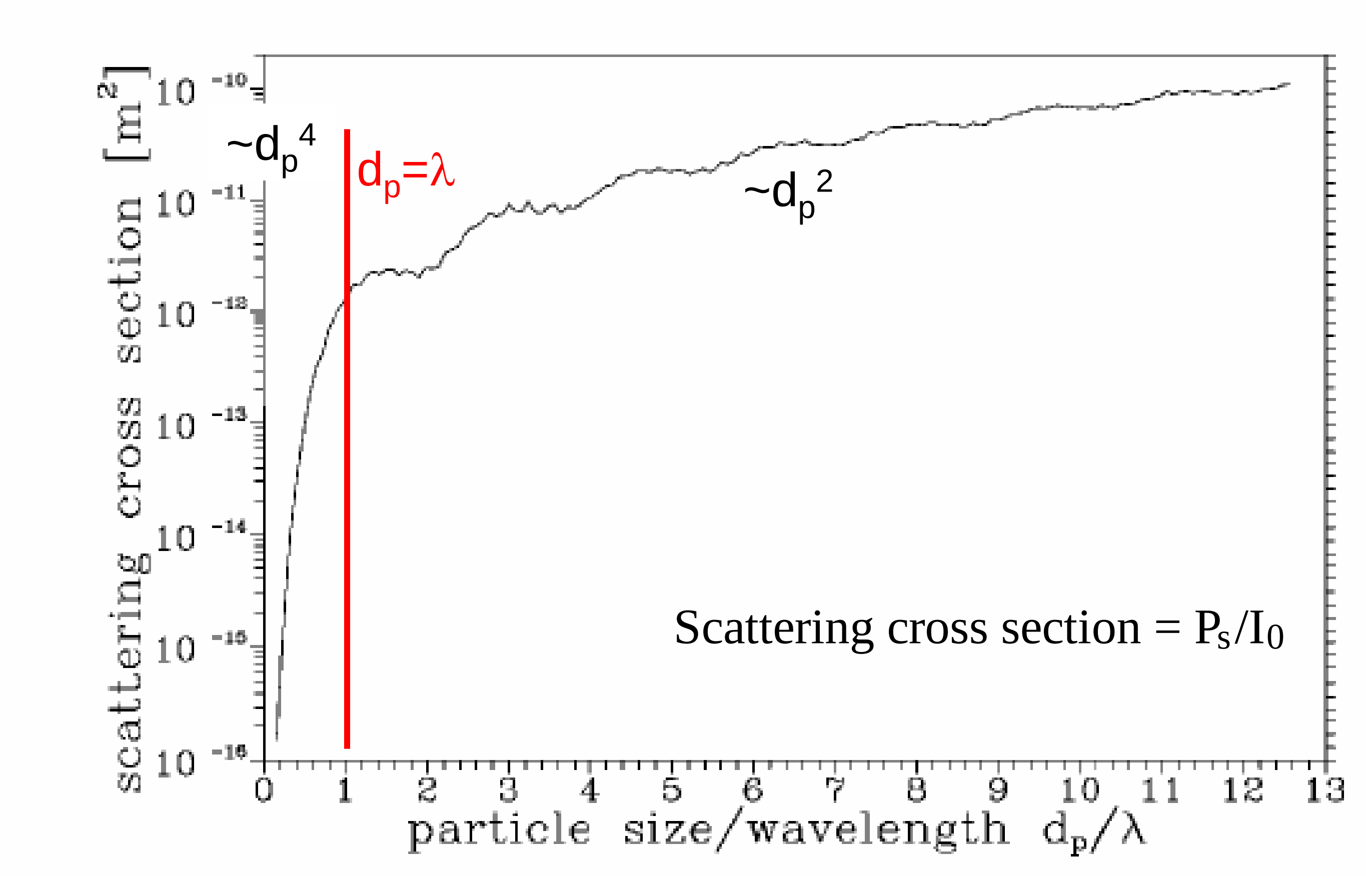

SEEDING (light scattering)

- LIGHT SCATTERING FROM SMALL PARTICLES
  - Particles should scatter enough light to be recorded and to produce high contrast images
  - Light scattered by small particles is a function of
    - Ratio of the refractive index of the particles to that of the surrounding medium scattering efficiency ⇧ as this ratio ⇧
    - Particle size, shape and orientation
    - Light polarization and observation angles (for PIV usually 90°)
  - For $d_p > \lambda$ MIE's scattering theory apply
    - Light scatter is not uniform! If $q = \pi d_p / \lambda > 1$, approximately q local maxima appear in the angular distribution over the range from 0° to 180°
    - By increasing the particle size (i.e. $\pi d_p / \lambda$) the ratio of forward to backward scatter intensity will increase rapidly.

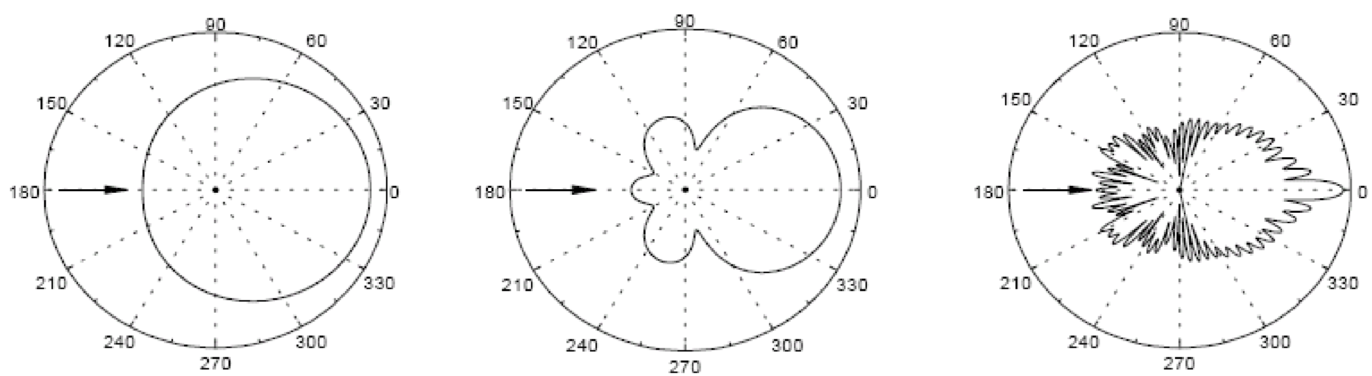

$d_p \cong 0.2\lambda$ $d_p \cong 1.0\lambda$ $d_p \cong 10\lambda$

Imaging of small particles

The image of a point source (scattering particle) does not appear as a point in the image plane of a camera, but forms a Fraunhofer diffraction pattern (Airy disk), even if it is imaged by a perfect aberration-free lens.

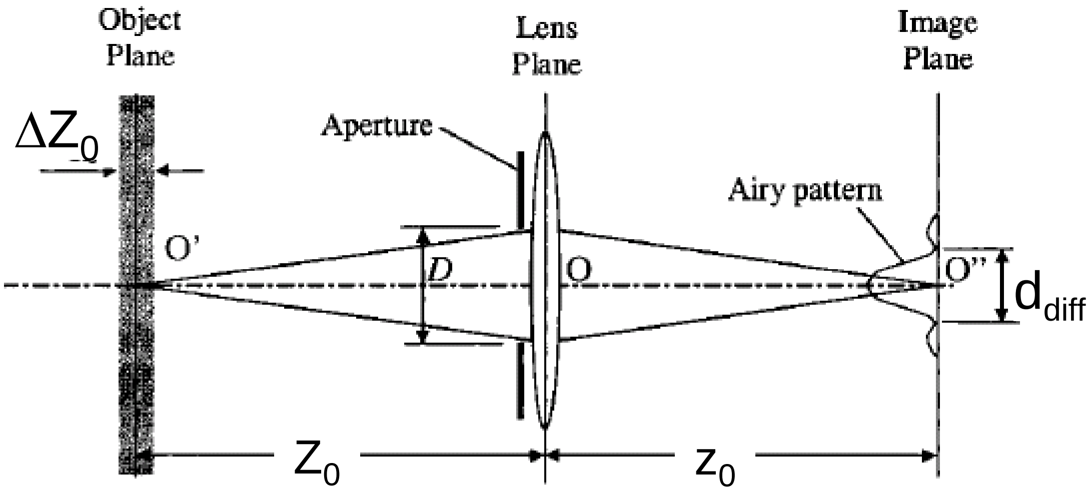

Figure 5. Diffraction effects during particle image recording.

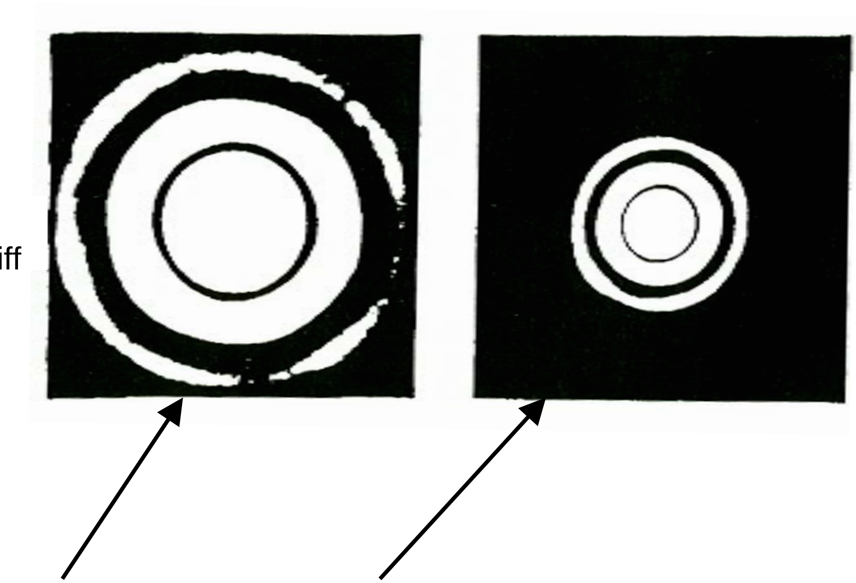

Airy pattern of a small and a larger aperture diameter

Imaging of small particles

The diameter, d_{diff}, of the Airy disk represents the smallest particle image that can be obtained by a given imaging configuration:

$$d_{diff} = 2.44 f_N (M+1)\lambda \qquad f_N = f / D$$

$M = z_0/Z_0$ magnification factor;
f = focal length of the lens; D = aperture diameter

The image of a particle is given by the convolution of the Airy disk and the geometric image of the particle ($d_g = M\, d_p$):

$$d_i = \sqrt{(Md_p)^2 + d_{diff}^2}$$

Normalized intensity distribution of the Airy pattern

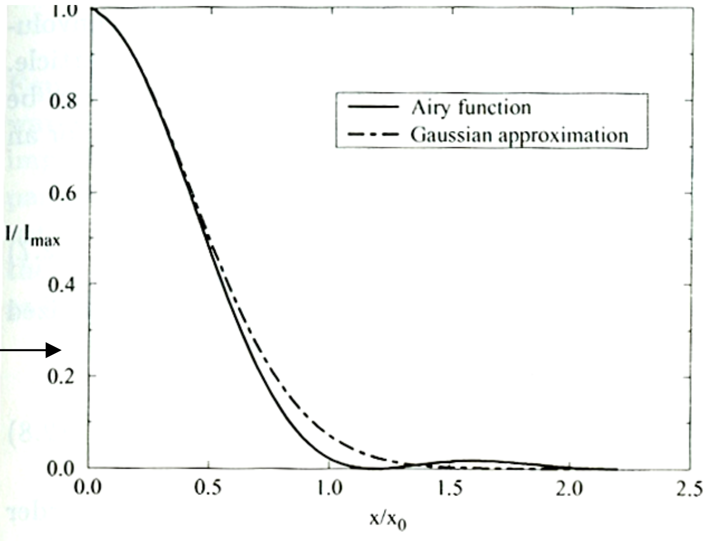

Imaging of small particles

Moreover, the particle-image diameter follows the previous equation for particle images in focus, i. e., when the light sheet thickness ΔZ_0 is smaller than the depth of field δ_z of the optical system given by:

$$\delta_z \cong 2 f_N d_{diff} \left(M+1\right)/M^2$$

Depth of field: is the region in which the image is "acceptably" sharp

M: image magnification, f_N: camera aperture, λ: laser wavelength

Using the diffraction limited image size of the particle

$$\delta_z \approx 4\left(1+1/M\right)^2 f_N^2 \lambda$$

For $M=0.1$, $f_N=5.6$, $\lambda=0.532\ \mu m \Rightarrow \delta_z \sim 8$ mm

Imaging of small particles

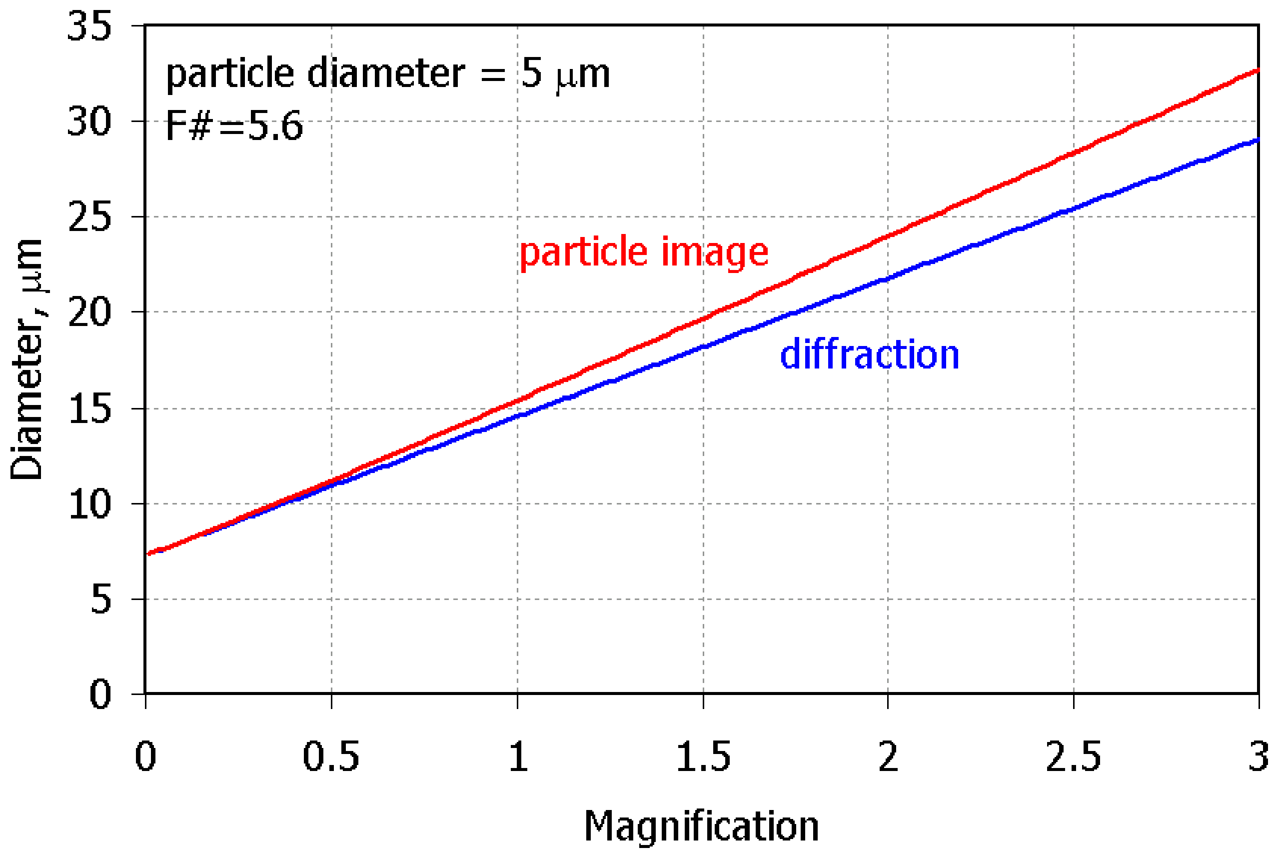

Since the lens is diffraction limited, the effective image diameter is larger and independent of particle size for $d_p < 10\ \mu m$

For $d_p > 50\ \mu m$ the image size is effectively the geometrical size

Actually image shape and size could differ from the Airy disk due to lens aberration

Particles Images on CCD

- Particle images size is usually diffraction limited (Airy Disk)
- Light distribution is approximately Gaussian
- Being image sampled by a CCD sensor, Nyquist criteria requires that to be properly resolved the (diffraction limited) particle image should cover at least 4 pixel

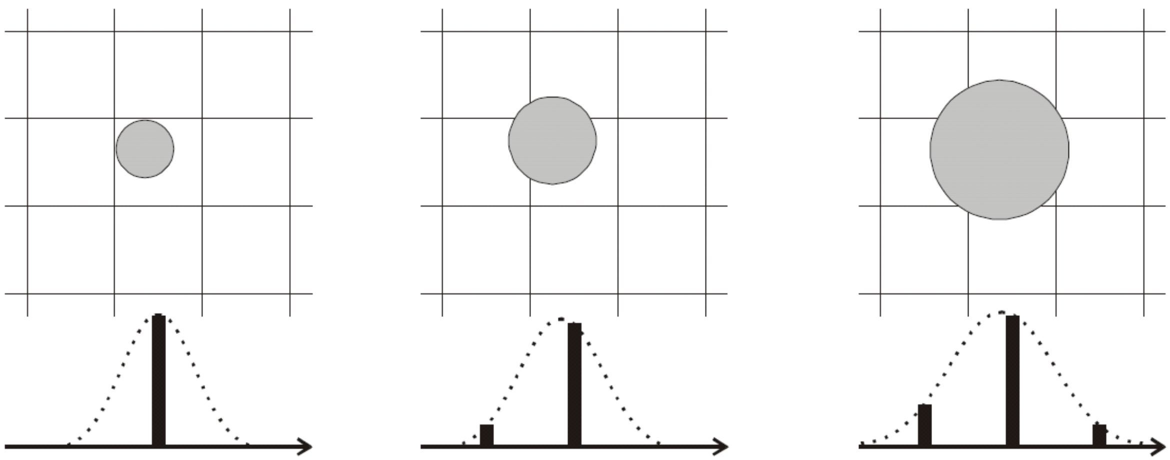

Particles Images on CCD

Digitized particle image:

Digital image
- pixel-by-pixel map of an image
- discrete 2D function

Gray value
- value to represent brightness: 0~255 (8-bit), 0~4095 (12-bit)

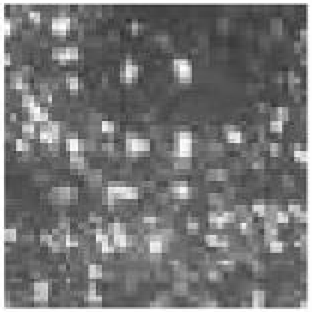

Gray value distribution
- Particle image with Gaussian profile (I_p)
- Single pixel random noise, e.g. thermal noise (I_{sp})
- Low frequency background noise (I_{lf}): non-uniform illumination, flow boundary etc.
- Total intensity distribution (I_{tot}): root-sum-square (RSS) of I_p, I_{sp} and I_{lf}

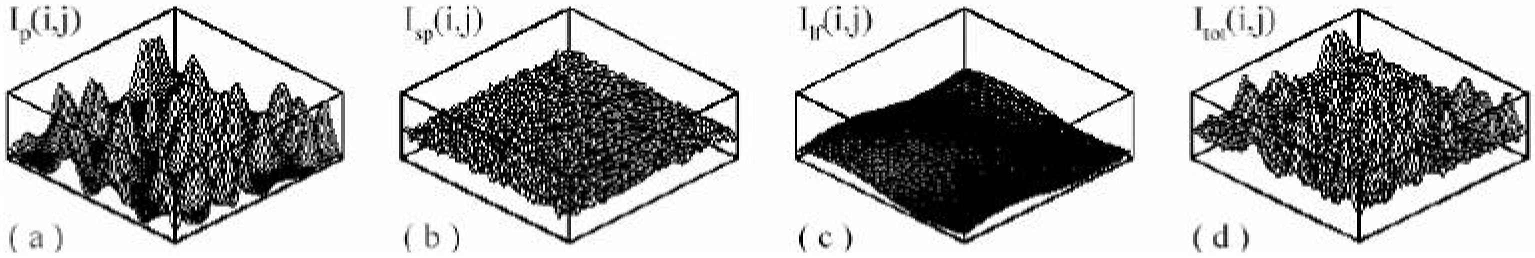

Components of PIV System
Light Sources

- **LASER** (stimulated light emission in an optically active media)
  - Solid state
  - Dye Laser
  - Gas
  - Semiconductor
- **GAS-DISCHARGE** (spontaneous light emission from excited gas molecule)
  - Xenon arc lamp (white light, pulsed, continuous, high power, used to simulate sunlight)
  - Deuterium arc lamp (strong UV source)
- **INCANDESCENCE** (thermal radiation)
  - Tungsten halogen lamp (visible+IR emission, high operating temperature)
- **ELECTROLUMINESCENCE** (light emission due to recombination of electron-hole pair)
  - **LED** (monochromatic emission, high pulse frequency and short pulse duration, low power, no IR)
- ……

Components of PIV System
Light Sources – Laser Principle

- Laser is based on Light Amplification by Stimulated Emission of Radiation
- Population inversion ($N_2 > N_1$) is forced to take place in a active material by means of a pump mechanism (flash lamp, electrical discharge)
- Once population inversion is achieved stimulated emission rapidly increases and an highly collimated, monochromatic light beam is emitted

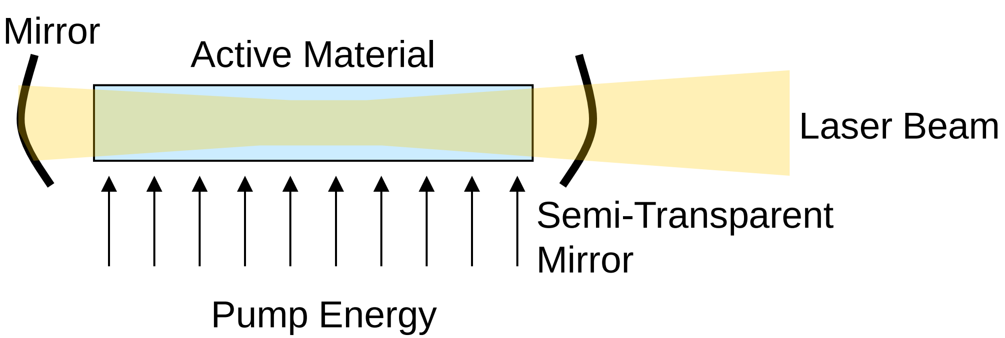

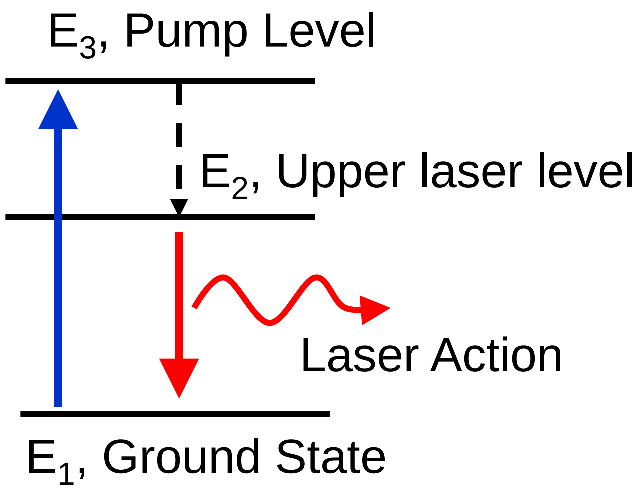

Components of PIV System
Light Sources - Lasers

- For the illumination it is preferable to use a laser, since the laser beam is easy to form into a sheet by a cylindrical lens.
- The laser must provide sufficient power to illuminate the seeds, and not so much that the camera becomes saturated (or damaged!).
- This usually leads us to the use of pulsed lasers, since one obtains a high light energy during a very short time interval (typically 5 ns for a YAG-laser). Particle images will be practically frozen even for high velocities (> 100 m/s).
- If only low power is required and the camera is shuttered, a continuous laser can be used.

Components of PIV System
Light Sources - Lasers

Continuous

Relatively low power light (P_{max} = 0.01 – 50 W) of good beam quality, easy to set up and maintain

- ***Helium–Neon*,** $\lambda = 633$ nm
- ***Argon Ion*,** several wavelengths, 488 nm, 514 nm ..

Single Pulse

- ***Ruby***

  $\lambda = 694.3$ nm, high pulse energy 1J, two pulses 1 to 500 μs apart with one laser, 1 pulse each ~30 s)

Repetitive Pulse

- ***Nd:YAG*** (yttrium aluminum garnet,$Y_3Al_5O_{12}$, *heavily used in PIV, pretty cheap ~40 k€*)

  2nd harmonic $\lambda = 532$ nm, max pulse energy ~0.5 J, double pulse require 2 lasers, flash lamps 10-50 Hz, high repetition rate are also available 1-10 kHz @ 10 mJ

- ***Nd:YFL*** (yttrium lithium fluoride,$YLiF_4$, $\lambda = 527$ nm)

  high repetition rate 1-10 kHz @ 10 mJ

- ***Copper Vapour***

  very expensive!, high repetition rates: 10-100 kHz, low pulse energy ~ 10mJ

Semiconductors, Diode-pumped Solid State Laser (DPSS)

Components of PIV System
Light Sources - Double Nd:YAG laser

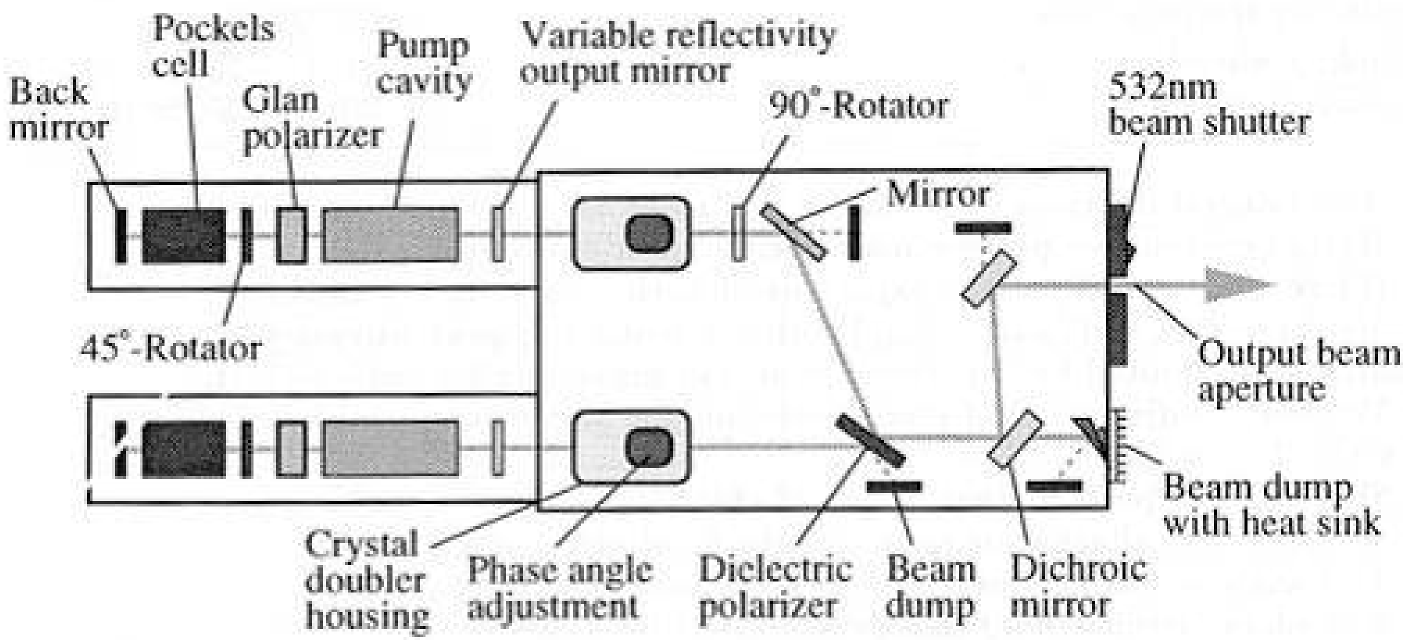

Fig. 2.17. Double oscillator laser system with critical resonators

The repetition rate of a YAG-laser is typically 10-30 Hz, which is too low except for very low velocities (< 1 cm/s). One therefore needs two lasers to get full freedom in terms of time separation between the pulses. Special PIV YAG-lasers are available that combine two laser cavities with a common beam outlet.

Components of PIV System
Light Sources – Laser Safety Issues

- ***SOME LASER SAFETY ISSUES***

  A typical Nd:Yag laser pulse has a energy of 0.01 to 0.5 J delivered in about 10 ns….this means 1-50 MW of laser beam peak power!!!

  - *Laser light can be VERY dangerous !!!*
  - *Even laser light reflections can be VERY harmful to eyes !!!*
  - *Eye damage depend upon laser power/energy and wavelength*
  - *Pulsed laser light at rate below 50 Hz can be quite harmful*

- ***SOME VERY BASIC SUGGESTIONS***

  - *Wear goggles*
  - *Operate at low laser light level and bright ambiance for all alignments*
  - *BE WISE!*
  - *Follows regulations!*

This section is not exhaustive!! it is given just to highlight safety issues!

Components of PIV System
Light-Sheet Formation Optics

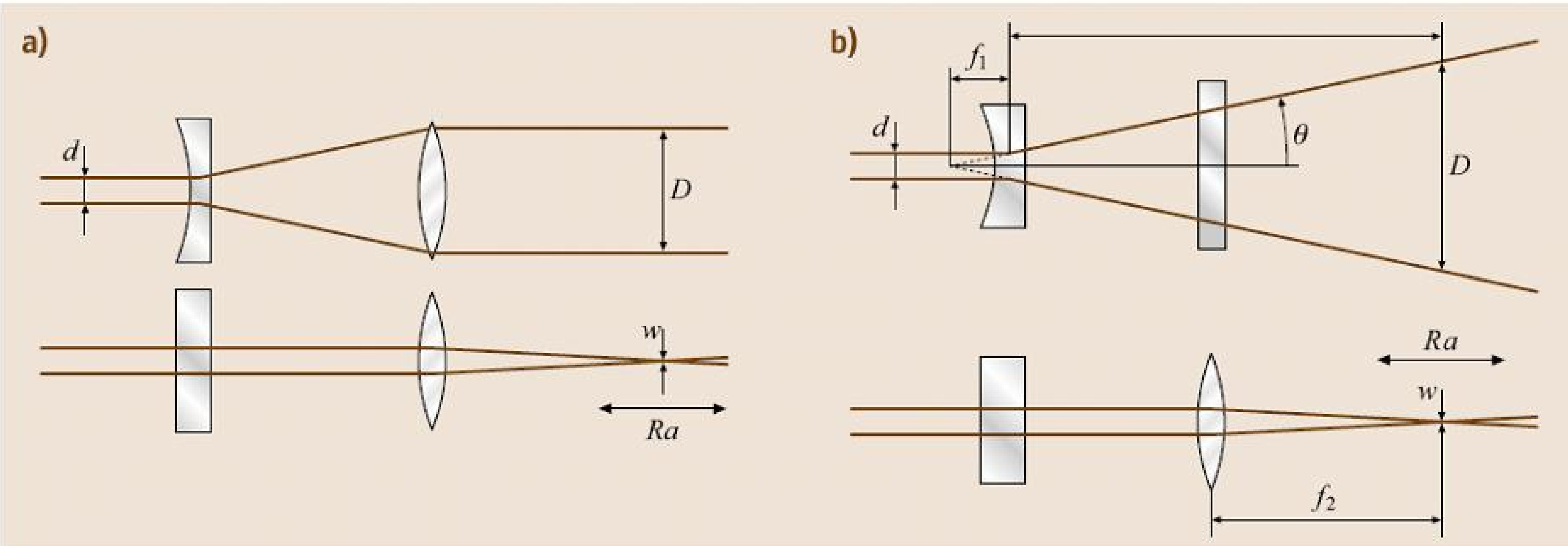

a) constant sheet width b) linearly expanding sheet width

- Due to beam divergence and diameter (~1 cm) one single lens is not sufficient to provide a thin laser sheet when using Nd-Yag laser
- Lens configuration can be chosen by using geometrical optics laws

The Rayleigh length Ra is the length over which the light sheet has a minimum thickness *w*

Components of PIV System
Image Recording Systems

- The positions of particles entrained in the flow is recorded by a camera, which is oriented 90 degrees to the plane of the light sheet.

- Early PIV was done on photographic film.

- Film still offers superior resolution and can be more sensitive but film limits the user to autocorrelation measurements, which introduces directional ambiguity.

- ***Charge coupled device (CCD) most widely used***. Most CCD cameras frame at video rates (30 frames per second, of Hz). Often, this is not fast enough. As a result, many PIV cameras use "frame straddling": The main challenge in frame straddling is getting the data from the first shot off the camera before the next one is taken. This is why PIV camera cost more

- Obviously pixels means resolutions. Bit depth means sensitivity and less limitation to the field of view and laser power.

Important considerations in camera choice:
Spectral response, spatial resolution, temporal resolution, dynamic range, cost

Components of PIV System
Cross-Correlation CCD Camera

To be able to acquire two single exposed images with a time separation of the order of micro seconds, one uses a so-called *full-frame interline transfer progressive scan* CCD camera, also called a *cross-correlation* CCD-camera.

The basic idea is that the image exposed by the first laser pulse is transferred very rapidly to light-hidden areas on the CCD-chip. This is done on a pixel-by-pixel basis, i.e. each pixel has its own storage site in immediate vicinity of the light sensitive pixel area.

After the second exposure, both images are transferred to the computer.

Since a lot of data has to be transferred, it is only possible to take a few double images per second.

The temporal resolution of the flow is thus in general very poor with this technique.

Components of PIV System
Cross-Correlation CCD Camera

- **CCD chip contains light sensitive cells and storage cells in an n by m array**
- **After the first exposure the image information is transferred to the storage cell and the CCD chip is ready for the second exposure**
- **Minimum time between cross correlation exposures is 200 ns.**

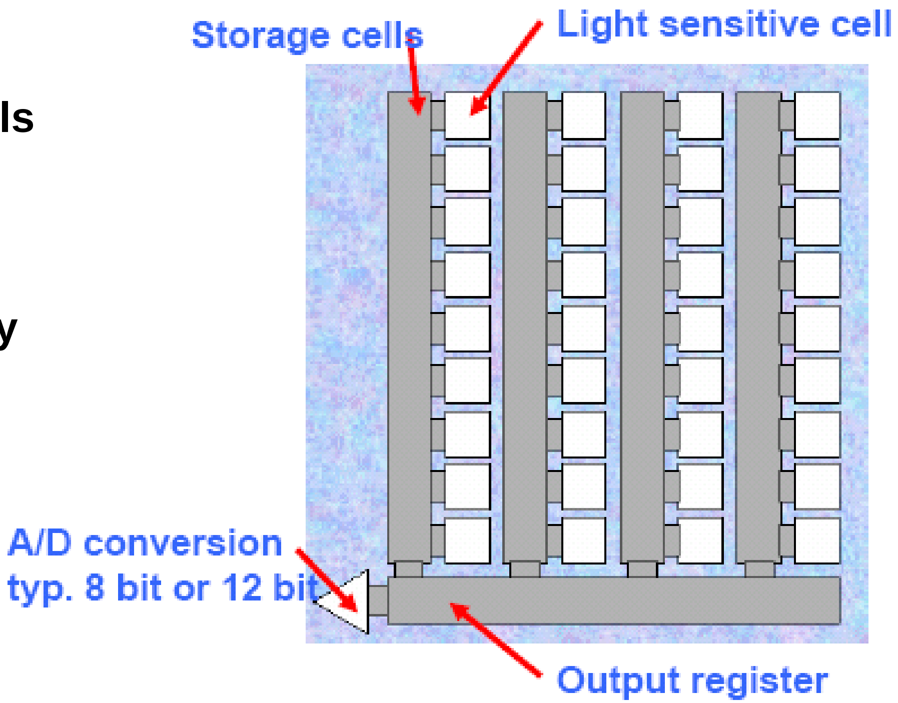

Electrons generated by impinging photon are continuously stored in the pixel site until read out

Components of PIV System
PIV with Cross-Correlation CCD Camera

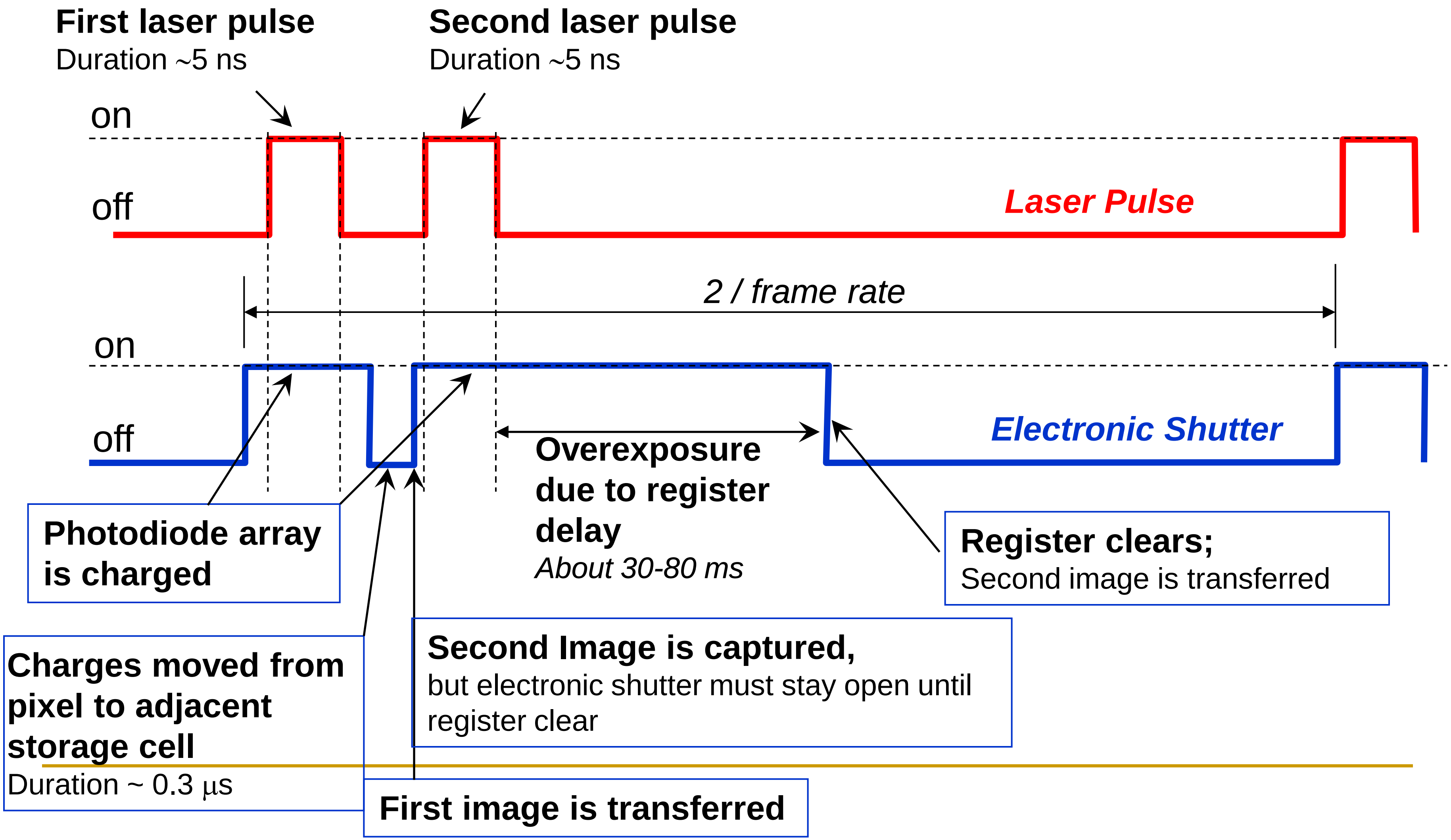

Components of PIV System
PIV with CCD Camera (general)

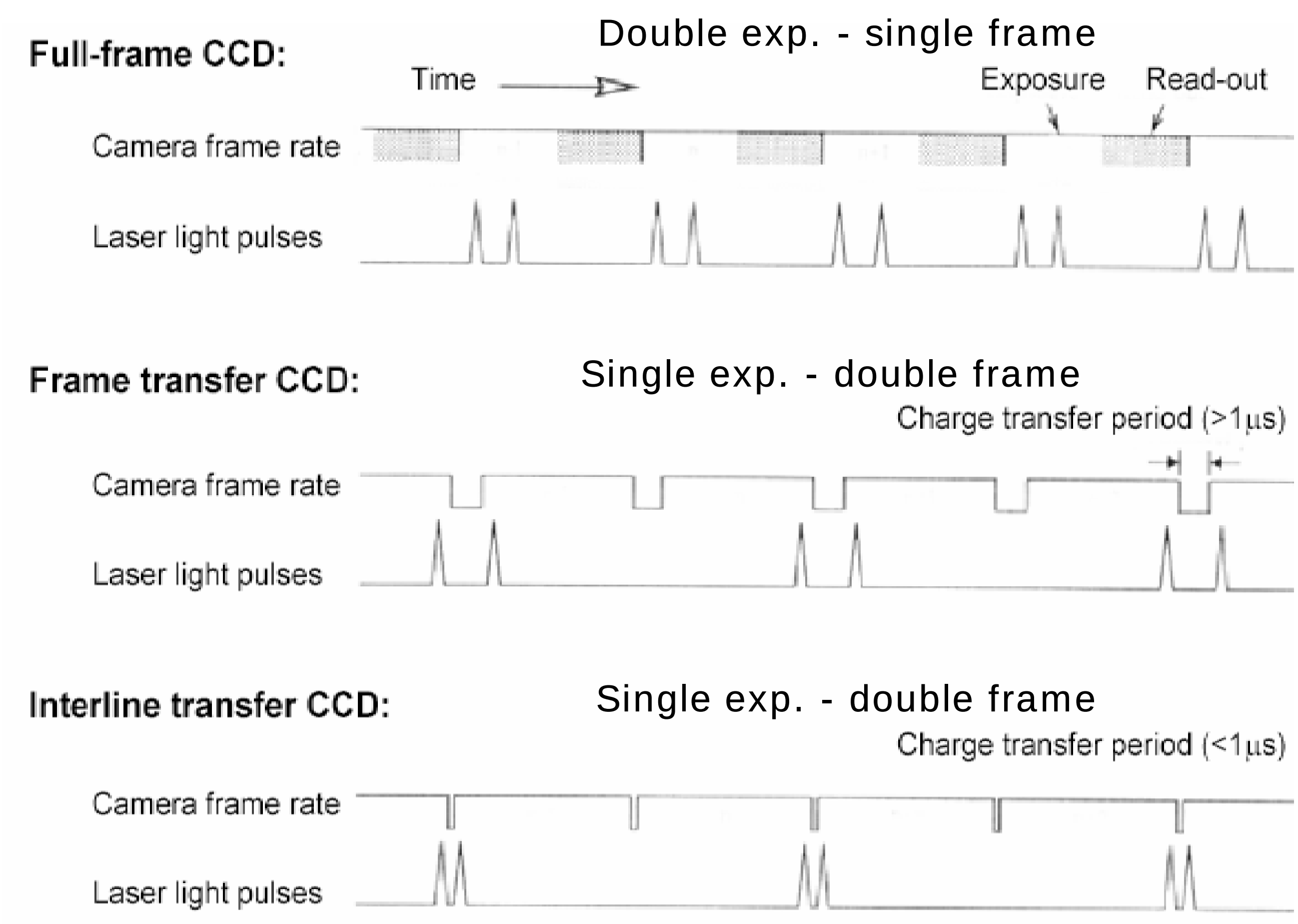

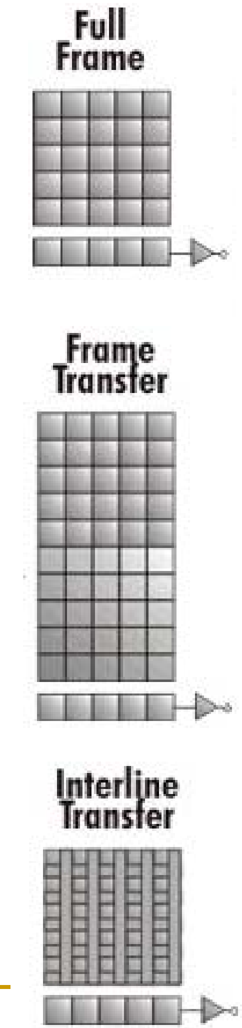

PIV frame rate is (camera frame rate)/2

Components of PIV System
Camera Optics

Typically, SLR lenses are used, and these also impact the results. Good quality lenses are mandatory to obtain accurate measurements.

The field of view and the working distance are functions of the camera optics.

Usually a narrow band filter is used in front of the lenses (or between lenses and camera) to block ambient light.

The Principle of PIV

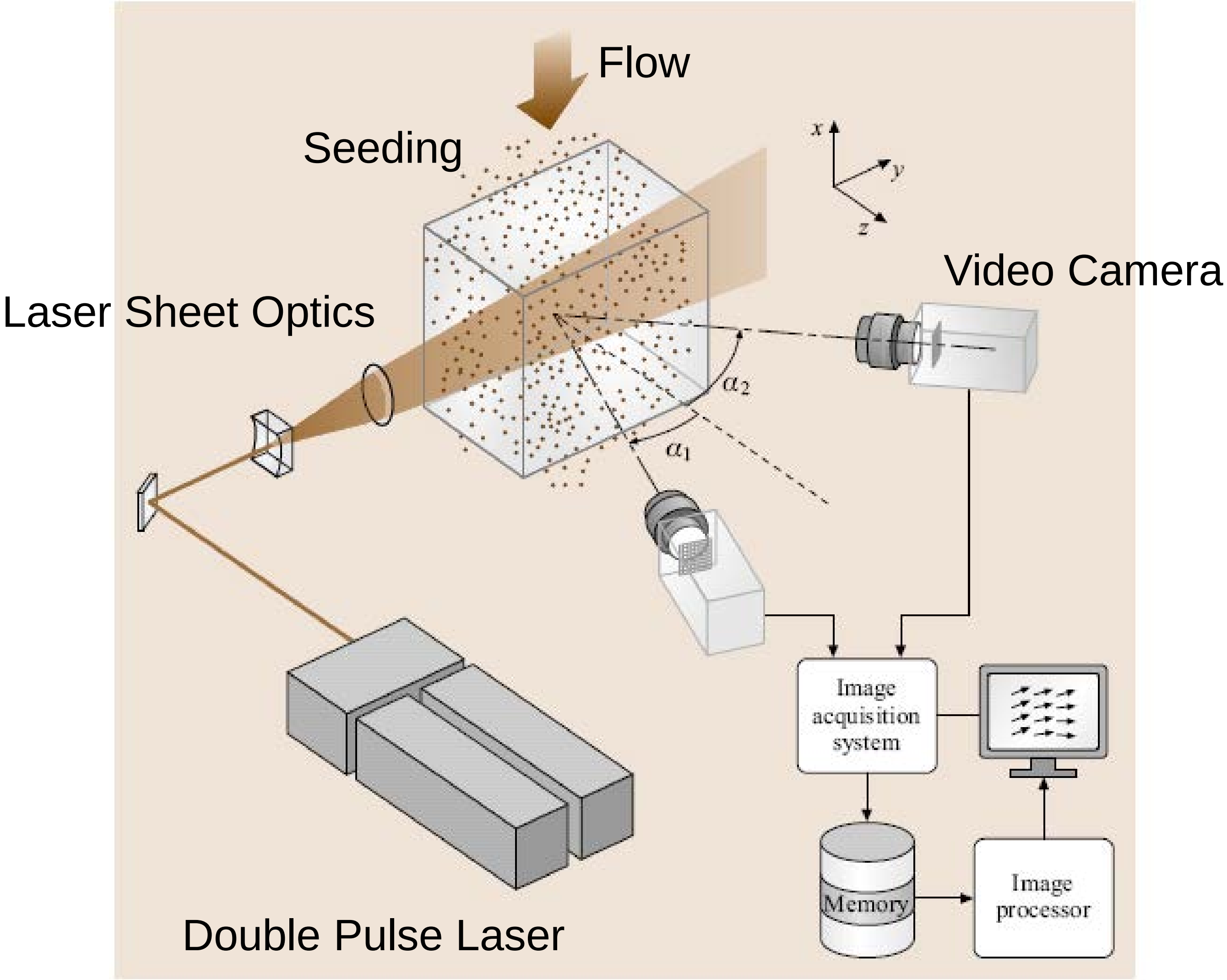

The Principle of PIV

Single Exposure – Double Frame

Two light pulses separated by short time interval

At each pulse the positions of particles are recorded using a digital or film camera (one pulse in one frame).

Two images are needed to evaluate the particle velocity.

Too long illumination times will result into streaks of the particle images that will not allow to determine the exact particle location in the fluid.

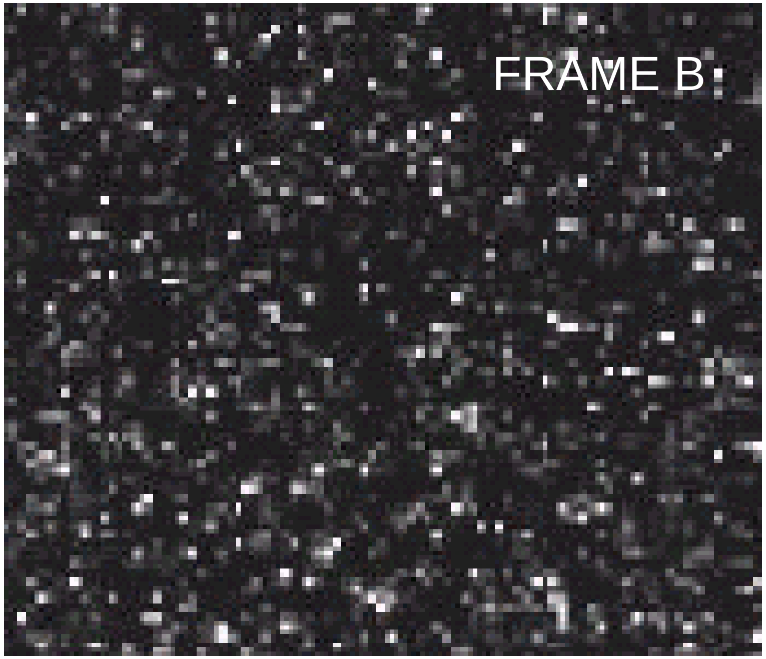

The Principle of PIV

Multiple Exposure – Single Frame

Two or more light pulses separated by a short time interval

At each light pulse the positions of particles are recorded using a digital or film camera (all pulses on a single frame).

Too long illumination times will result into streaks of the particle images that will not allow to determine the exact particle location in the fluid.

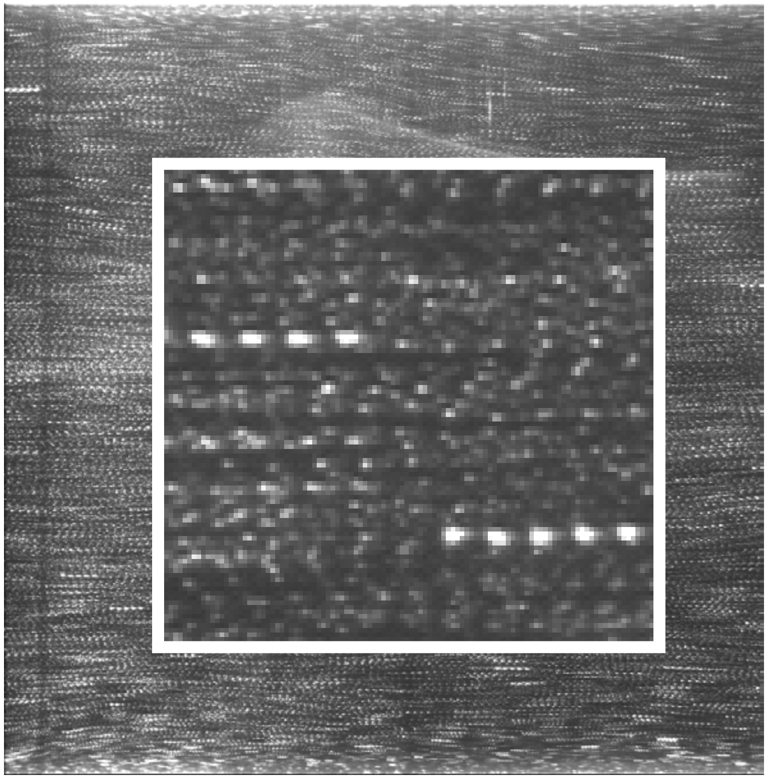

Analysis of PIV images
Optical set-up

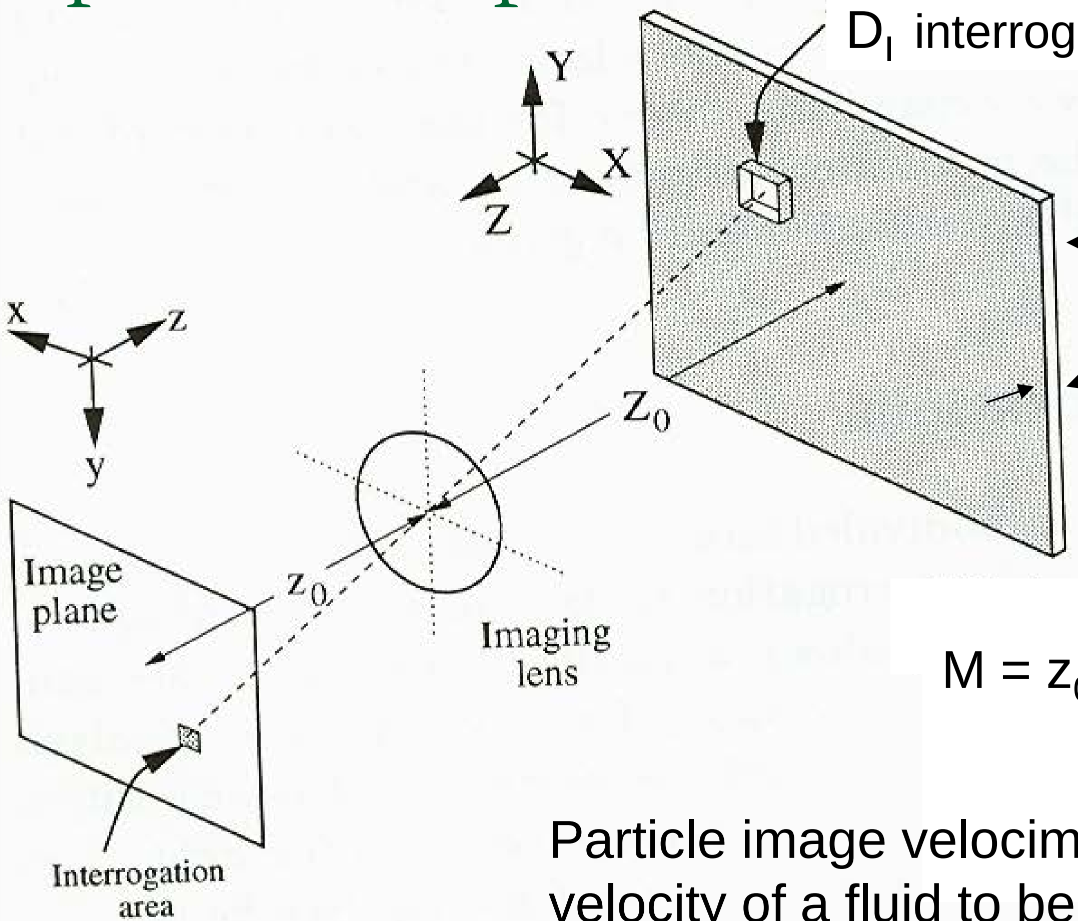

D_I interrogation-spot diameter

Object plane

ΔZ_0 light-sheet thickness

$M = z_0/Z_0$ image magnification

Particle image velocimetry (PIV) allows the mean velocity of a fluid to be measured in a small area D_I, illuminated by a light sheet and seeded with tracer particles of concentration C

Analysis of PIV images

PIV images are defined accordingly to their particle density

Particle density is represented by two dimensionless parameters:

- Image particle density N_I represents the number of individual particles in the “probe volume”.
- Source density N_S represents whether the particle images are overlapping ($N_S > 1$) or can be recognized individually ($N_S < 1$).

$$N_S = \frac{C\Delta z_0}{M_0^2} \cdot \frac{\pi}{4} d_\tau^2$$

$$N_I = \frac{C\Delta z_0}{M_0^2} \cdot D_I^2$$

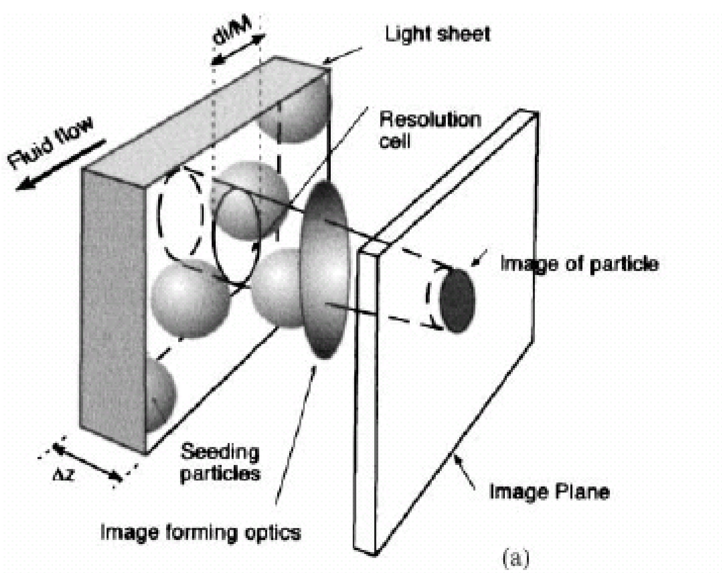

(a)

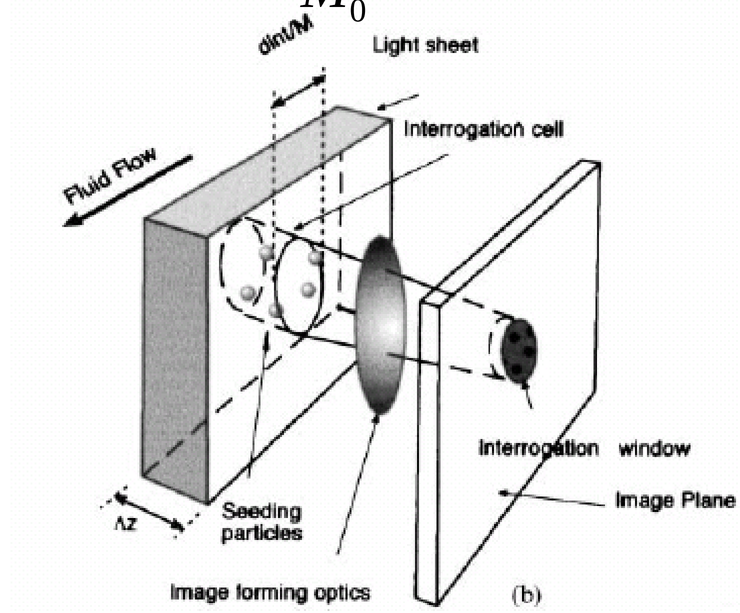

(b)

Analysis of PIV images

Particle density defines the type of velocimetry that can be used:

- Particle Tracking Velocimetry (PTV)
- Particle Image Velocimetry (PIV).

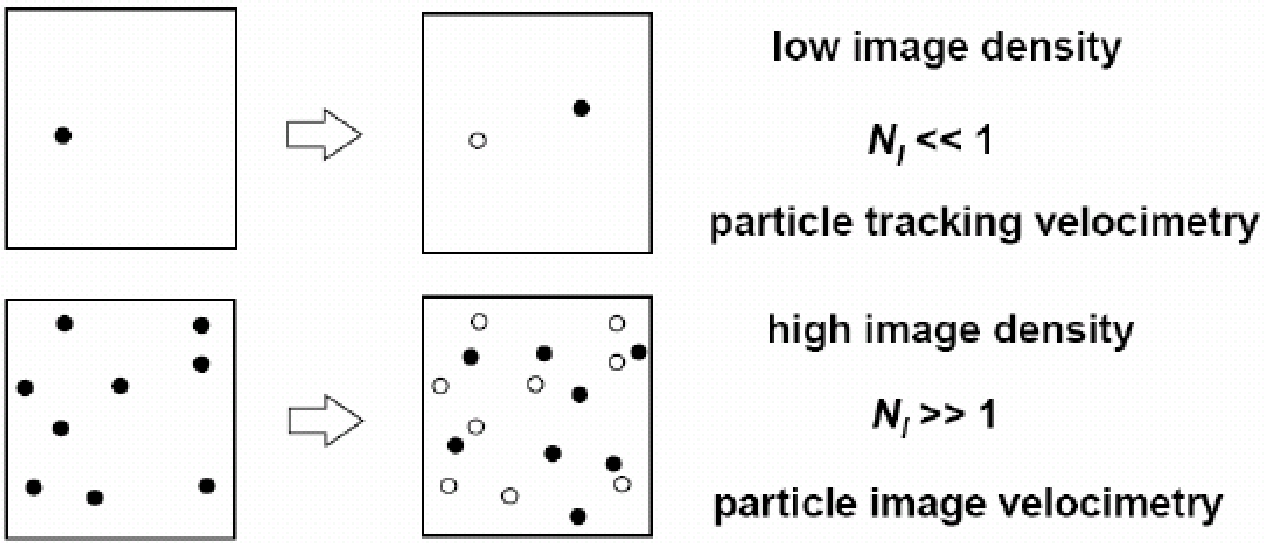

Respect to low-image density PIV the interrogation in any location normally contains sufficient particle images to obtain a valid measurement.

In general, the number of velocity data extracted from high-image-density PIV is an order of magnitude larger than for low-image-density PIV

Analysis of PIV images

Several recording strategies can be implemented

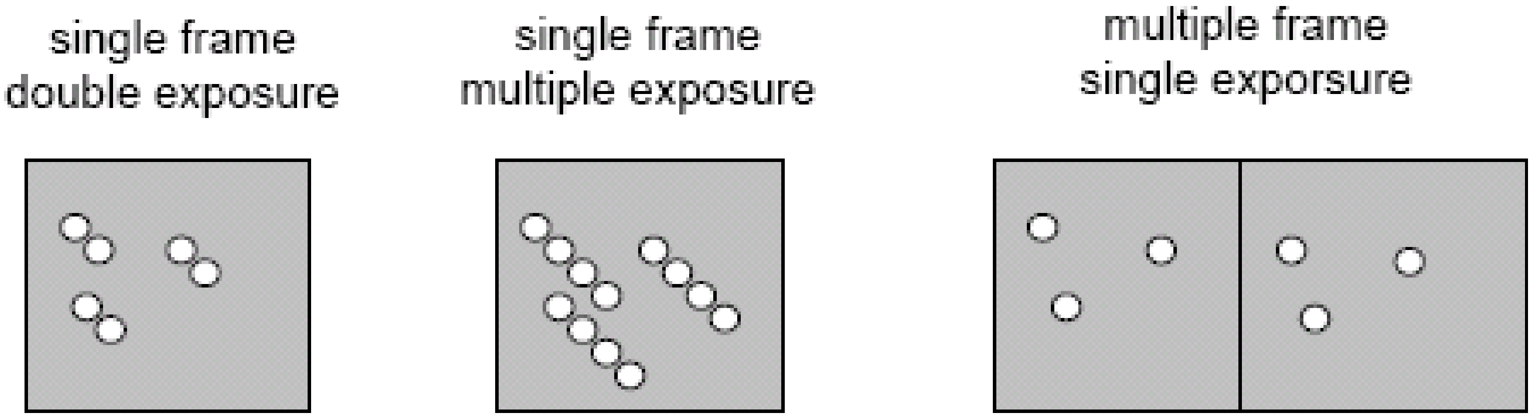

Since it is impossible to track the individual particles, the *mean* displacement of particles in a small region of the image(s) (the interrogation area) has to be calculated by a numeric algorithm, es. spatial correlation in case of digital PIV (DPIV).

Analysis of PIV images
Double exp-single frame (Autocorrelation)

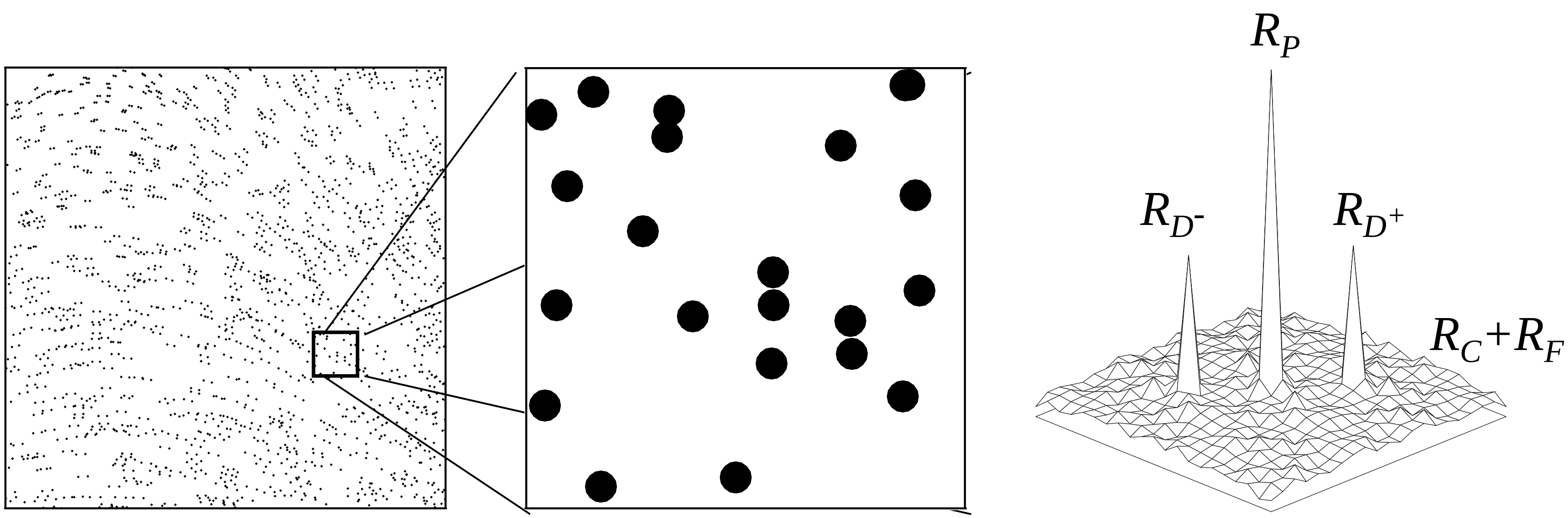

Double-exposed image

Interrogation region

Spatial correlation

Analysis of PIV images
Double exp-single frame (Autocorrelation)

For a double exposed image, the auto-correlation algorithm is applied to a small interrogation area (D_I) of size MxN. the ***auto-correlation*** function is given as

$$\Phi(m,n) = \sum_{i=1}^{M}\sum_{j=1}^{N} I_1(i,j)\cdot I_1(i+m,\, j+n)$$

where I_1 is the grey value distributions

Auto correlation show ***one peak at zero displacement*** and two mirrored displacement peaks.

The mean particle image displacement in the interrogation area is determined by the position of the max value of Φ(m,n).

Auto correlation cannot resolve directional ambiguity by itself.

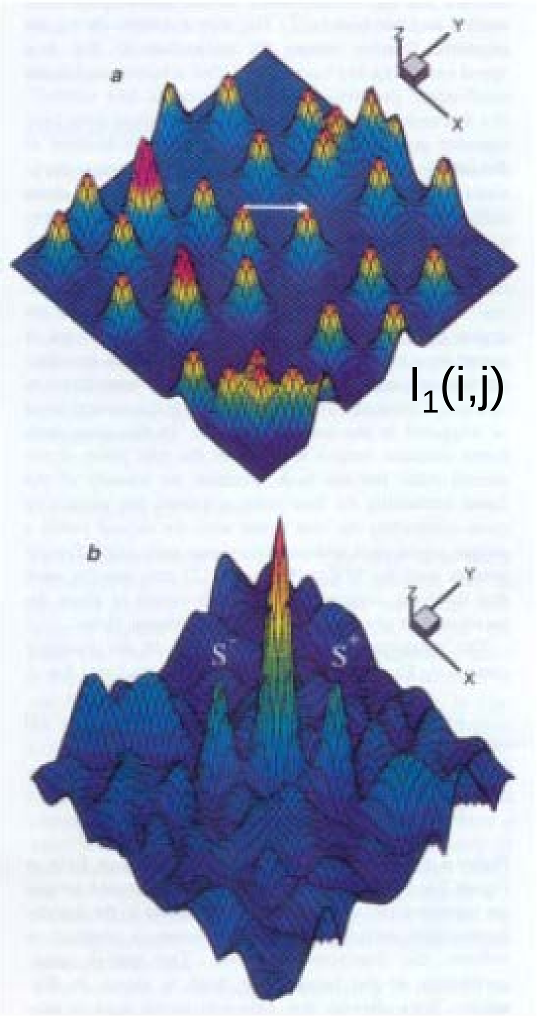

Autocorrelation field

Analysis of PIV images
Single exp–double frame (Cross-correlation)

Cross-correlation algorithm using two images of particles in the flow is used for calculating the velocity vector

The 2-D average particle motion is obtained by correlating the interrogation area's of the two images.

$$\Phi(m,n) = \sum_{i=1}^{M} \sum_{j=1}^{N} I_1(i,j) \cdot I_2(i+m, j+n)$$

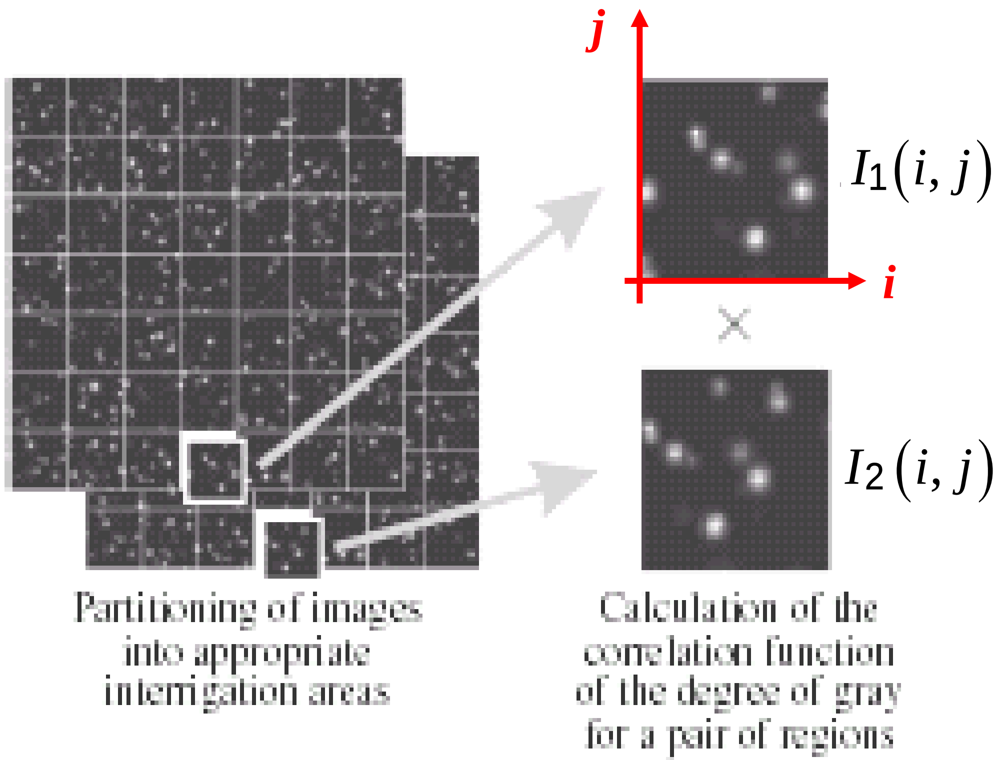

- *m and n* are shifts of the second IA respect to the first one

Analysis of PIV images
Single exp–double frame (Cross-correlation)

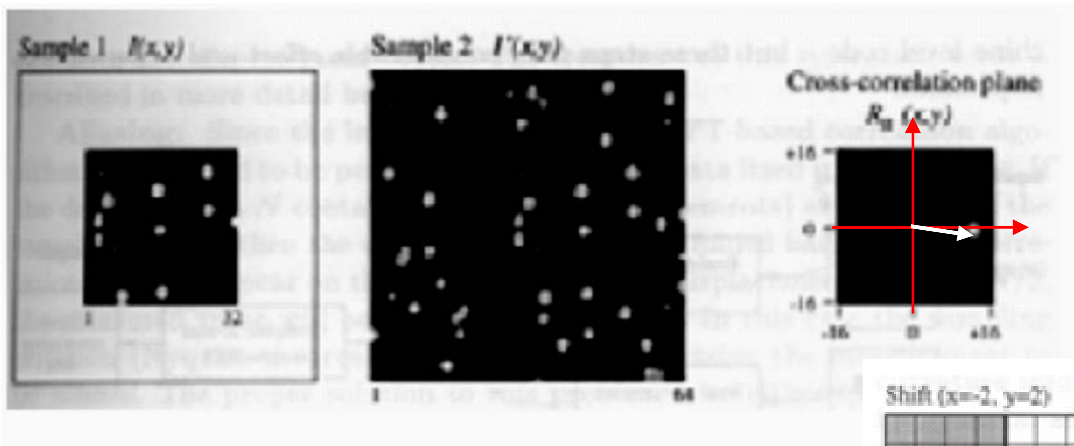

Average particles displacement is given by position of the peak

The cross-correlation method contains two assumptions:

1) The contribution from noise is negligible
2) The particles within the interrogation area move uniformly in a single direction during their double image capturing time

Since velocity gradients may prevent the validity of the 2nd assumption, a condition on the velocity variation is recommended

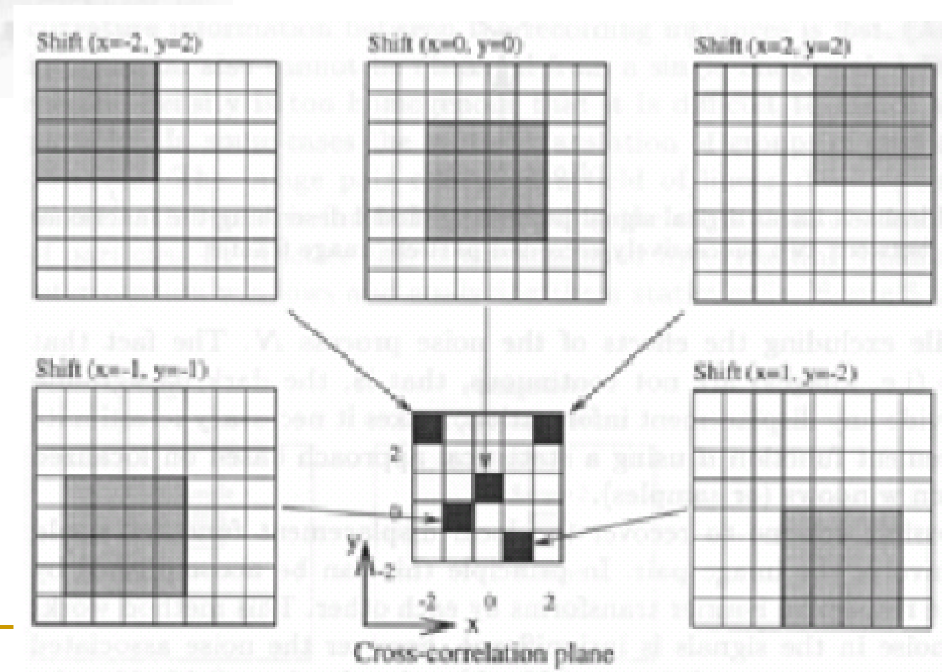

CROSS-CORRELATION PROCEDURE

Analysis of PIV images

Single exp–double frame (Cross-correlation)

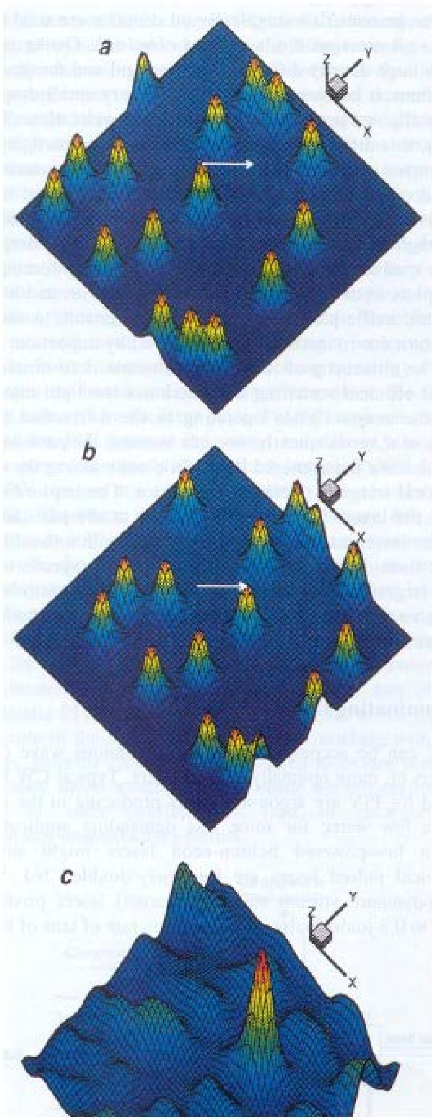

For a single exposed PIV recording pair, the cross-correlation algorithm is applied to a small interrogation area (D_I) of size MxN. Two samples are chosen, from the first and second images and the *cross-correlation* function is given as

$$\Phi(m,n) = \sum_{i=1}^{M} \sum_{j=1}^{N} I_1(i,j) \cdot I_2(i+m, j+n)$$

where I_1 and I_2 are grey value distributions

The mean particle image displacement in the interrogation area is determined by the position of the max value of Φ.

Cross correlation renders only the velocity peak.

Cross correlation resolves directional ambiguity by using two consecutive images.

Analysis of PIV images
Single exp–double frame (Cross-correlation)

Mean Intensity Fluctuating Displacement

$$\Phi = R(\mathbf{s}) = R_C(\mathbf{s}) + R_F(\mathbf{s}) + R_D(\mathbf{s})$$

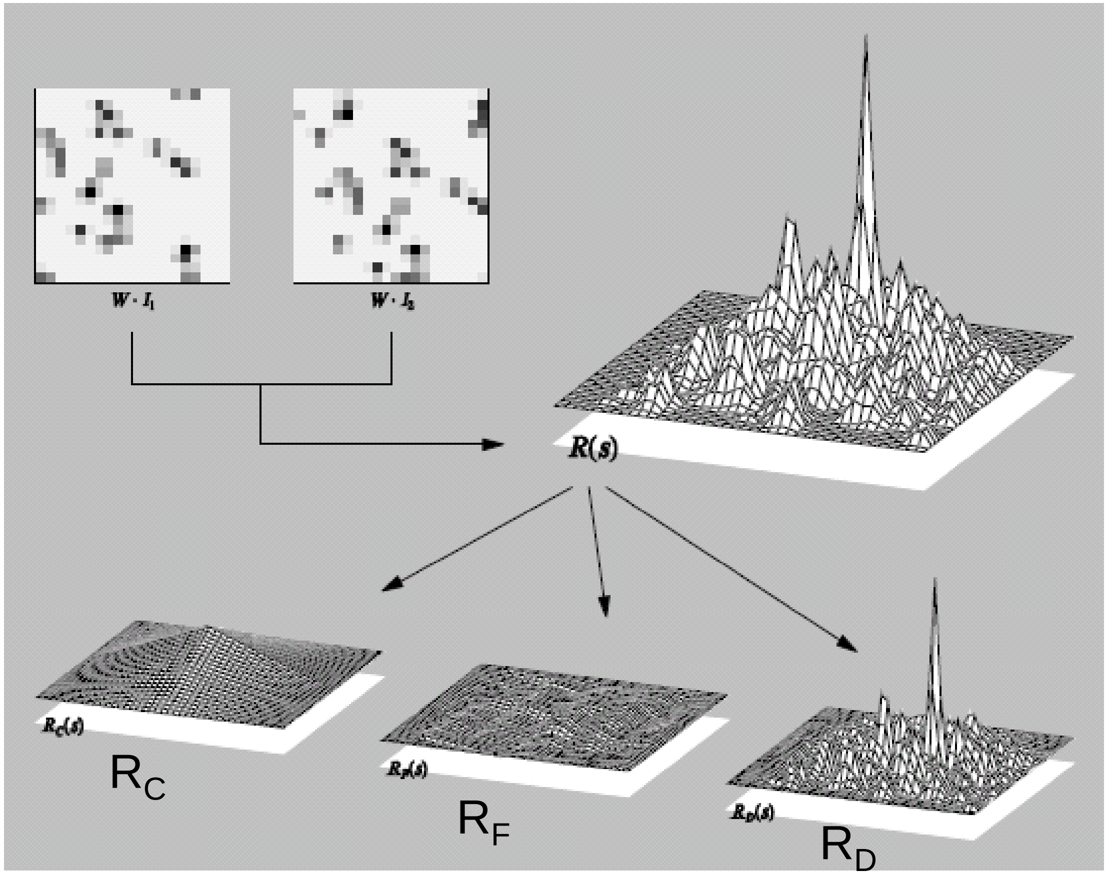

Analysis of PIV images
Single exp–double frame (Cross-correlation)

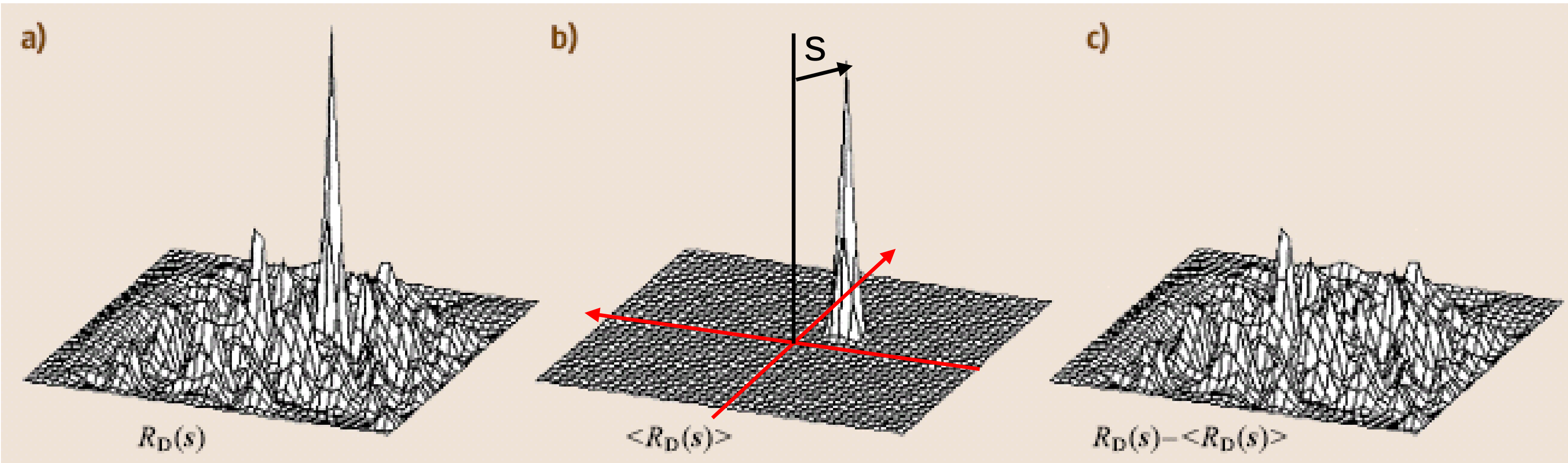

Fig. 5.102a–c Separation of the displacement-correlation term R_D (**a**) into mean (**b**) and fluctuating terms (**c**)

Displacement   Noise

$$R_D(s) = \langle R_D(s)|u\rangle + R'_D(s)$$

The correct displacement-correlation peak can be identified only when its amplitude is larger than the highest random correlation peak in $R'_D(\boldsymbol{s})$.

Otherwise the interrogation analysis yields a *spurious* value for the particle-image displacement.

The ratio of the highest correlation peak and that of the second highest correlation peak is a measure of the *detectability* of the displacement-correlation peak, indicated by D_0, and can be considered as a lower limit of the signal-to-noise ratio.

Analysis of PIV images
Particle Pair Loss

IN-PLANE LOSS (F_I)
Particle pair are lost due to particle in-plane displacement to laser sheet.

OUT-PLANE LOSS (F0)
Particle pair are lost due to particle displacement perpendicular to laser sheet.

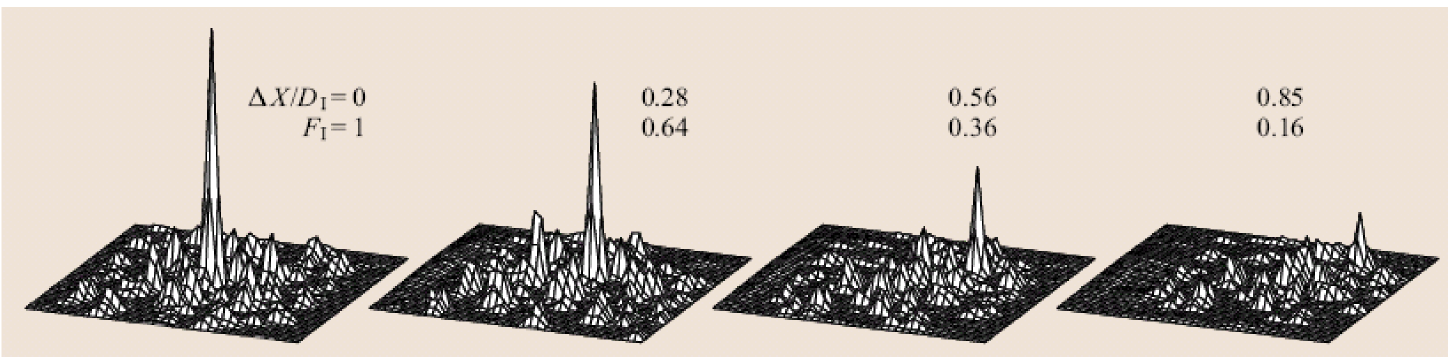

Fig. 5.104 The spatial correlation for increasing in-plane displacement (at constant image density)

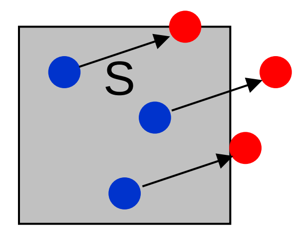

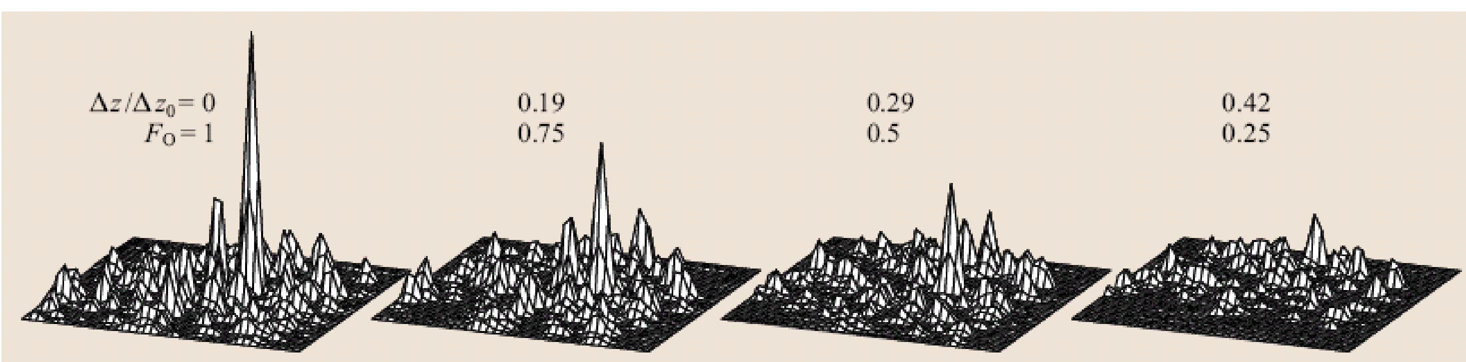

Fig. 5.105 The spatial correlation for increasing out-of-plane motion

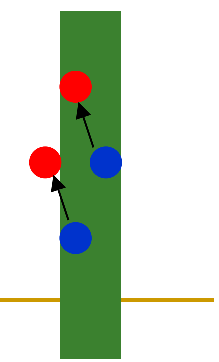

Laser sheet

Analysis of PIV images
Correlation based techniques

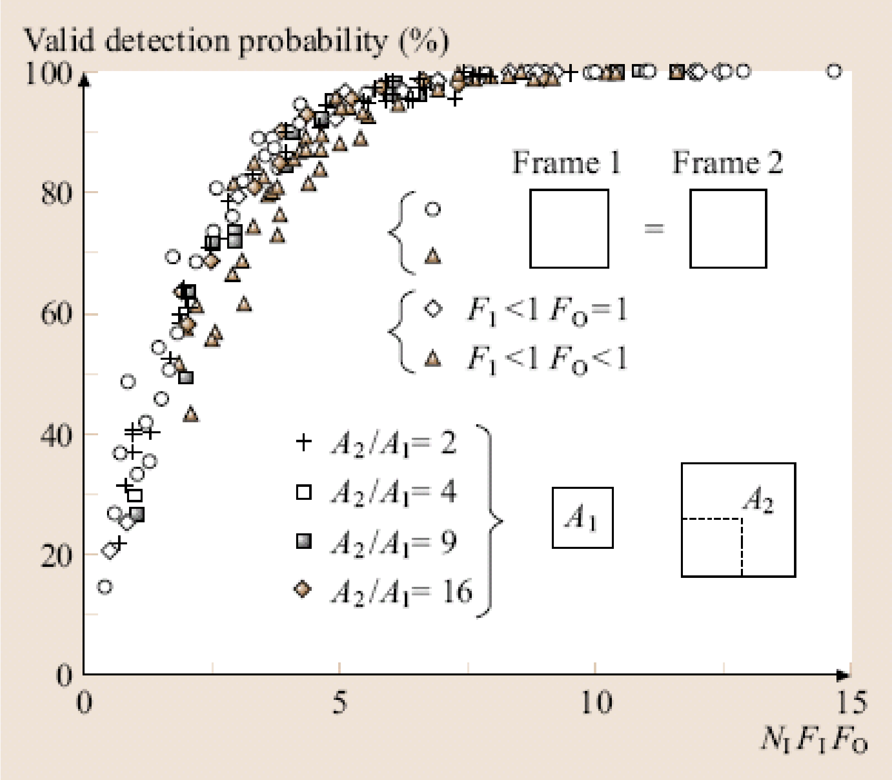

Fig. 5.107 The valid detection probability for the displacement-correlation peak as a function of the image density N_I and the in-plane and out-of-plane loss of correlation, F_O and F_I, respectively (after *Keane* and *Adrian* [5.434])

N_I = image density
F_I = in plane loss of images
F_O = out of plane loss of images

If the value of $N_I F_I F_O$ is above 5 the probability to make a valid measurement is above ~90%

Analysis of PIV images
Sub-Pixel Resolution

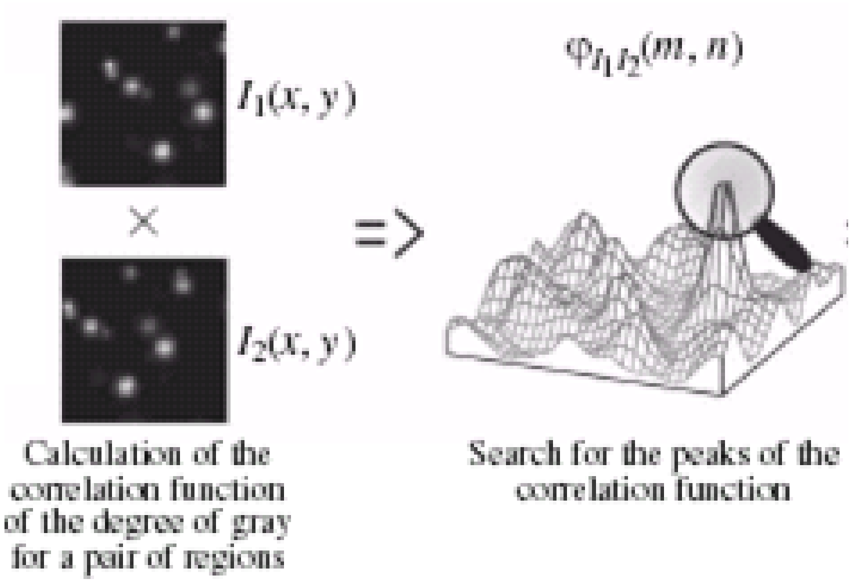

- The displacement obtained by cross-correlation (auto-correlation) algorithms is resolved within ±0.5 pixel (error could be as large as 1 pixel).
- Under this circumstance the relative error for digital PIV measurements would not be better than 1/8(≈ 13%) when using an IA of 32x32 pixels and a displacement of 8 pixels
- A sub-pixel resolution can be achieved by interpolating the discrete cross-correlation (auto-correlation) function (uncertainty ~0.05–0.10 pixel)
- Intensity distribution of particle image has a Gaussian shape, a Gaussian fit is applied to the 3 adjacent points of Φ (along x and y)

Analysis of PIV images
Sub-Pixel Resolution

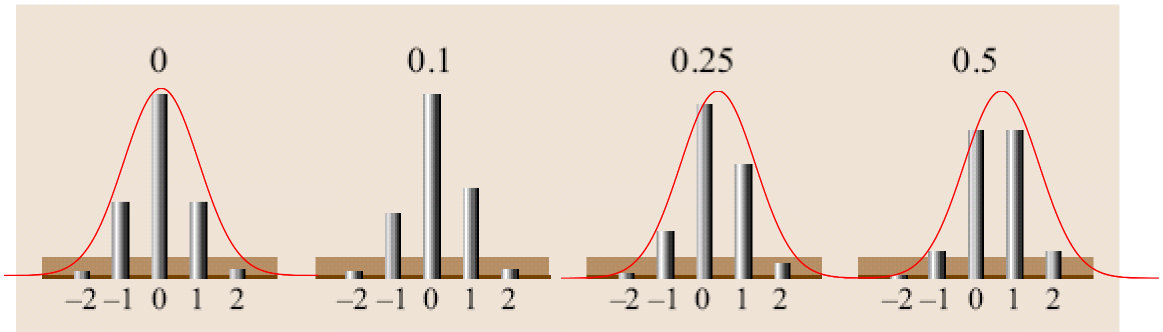

Fig. 5.108 Detailed shape of the correlation peak (in one dimension) as a function of the subpixel part of the displacement (here shown for a 1.6 pixel particle-image diameter). The *horizontal shaded region* represents the background noise level in the correlation

Gaussian Intensity distribution

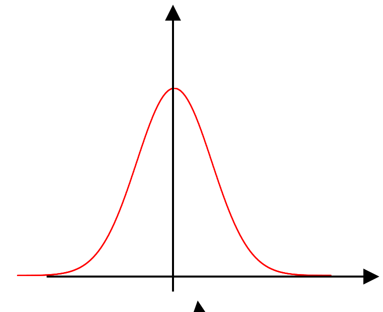

$$\boxed{I(X, Y; t) = \frac{2\alpha}{\frac{\pi}{4} d_\tau^2} \exp\left[-8\frac{(X - X_0)^2 + (Y - Y_0)^2}{d_\tau^2}\right]}$$

$$\hat{\varepsilon}_X = \frac{\ln R_{-1} - \ln R_{+1}}{2(\ln R_{-1} + \ln R_{+1} - 2\ln R_0)} \ ,$$

with

$$R_{-1} \equiv R_D[m_0 - 1, n_0], \ R_0 \equiv R_D[m_0, n_0],$$
$$R_{+1} \equiv R_D[m_0 + 1, n_0] \ ,$$

- A sub-pixel resolution can be achieved by interpolating the discrete cross-correlation (auto-correlation) function (uncertainty ~0.05–0.10 pixel)
- Intensity distribution of particle image has a Gaussian shape, a Gaussian fit is applied to the 3 adjacent points of F (along x and y)

Analysis of PIV images
Correlation based techniques FFT

- The computation of correlation is very expensive

  number of operation ~(MxN)^2 ~ 10^6

- Fast Fourier Transform (FFT) algorithm allows to speed up the correlation process (4MN $\log_2$MN, ~ 10^4)
- FFT could introduce artifact in $\Phi(m,n)$

$$\Phi(m,n)=\sum_{i=1}^{M}\sum_{j=1}^{N} I_1(i,j)\cdot I_2(i+m,j+n)$$

$$\begin{tikzcd}
I_1(i,j) \arrow[r, "\text{FFT}"] & \hat{I}_1(u,v) \arrow[rrd] & & \\
I_2(i,j) \arrow[r, "\text{FFT}"] & \hat{I}_2(u,v) \arrow[r] & \hat{I}_2^{*}(u,v) \arrow[r] & \hat{\Phi}(u,v)=\hat{I}_1(u,v)\hat{I}_2^{*}(u,v) \arrow[d, "\text{FFT}^{-1}"] \\
& & & \Phi(m,n)
\end{tikzcd}$$

Change sign of real part
Complex Conjugate

Analysis of PIV images
Single exp–double frame (Cross-correlation)

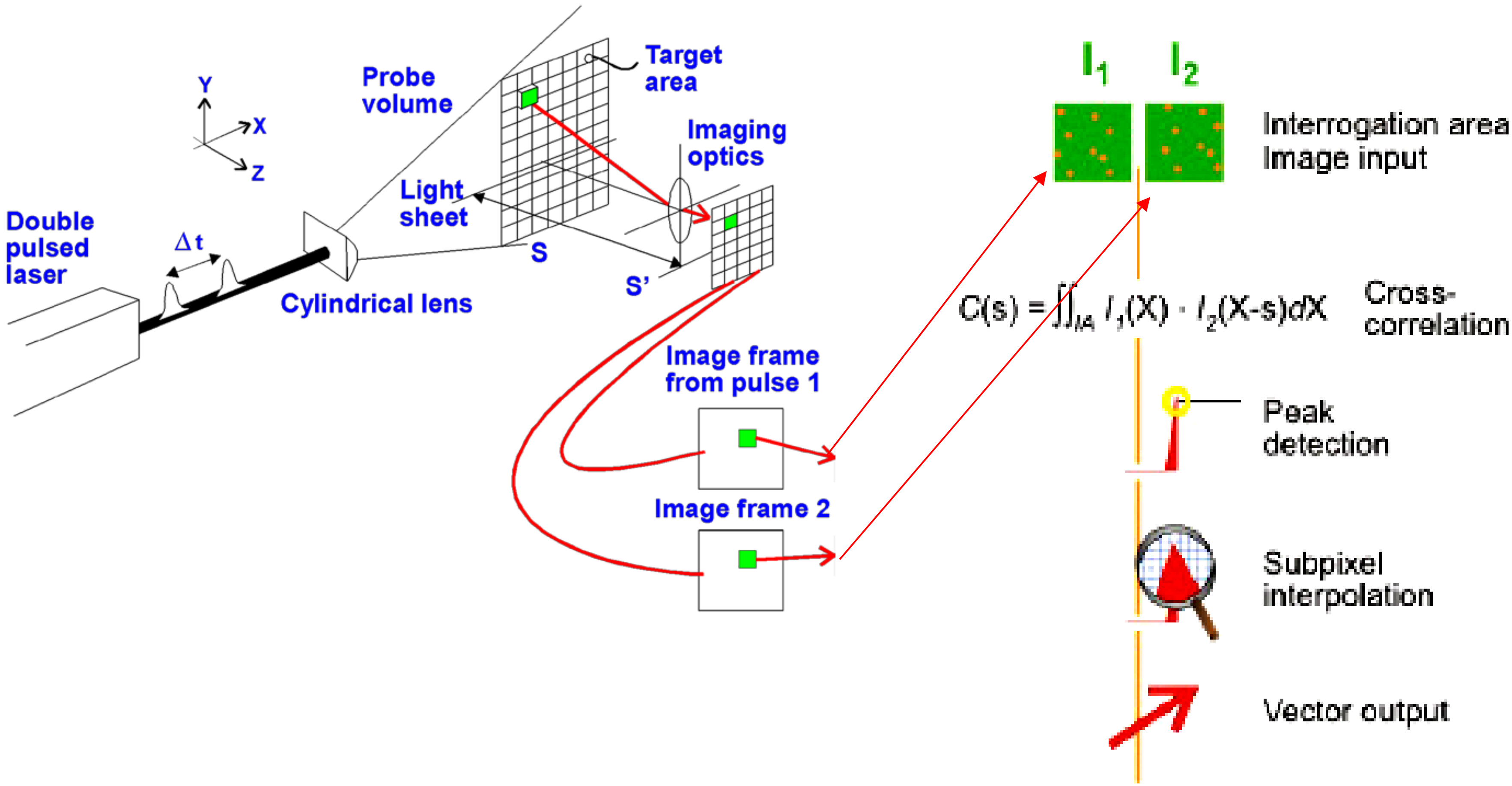

Performance of Correlation Techniques
Random Errors

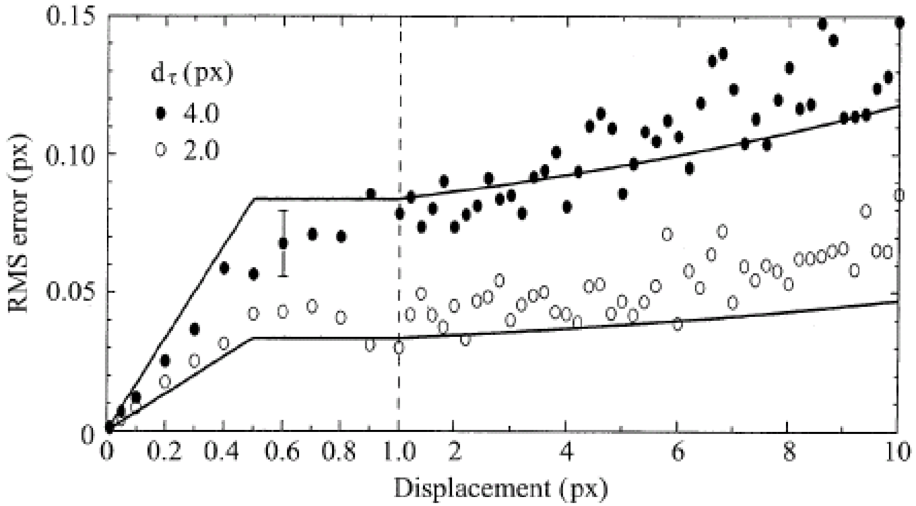

Fig. 1. The RMS estimation error for the displacement as a function of the displacement u in pixel units for a 32×32-pixel interrogation region in digital PIV cross-correlation analysis, for particle-images with a diameter of 2 and 4 pixels with an image density of 10, with zero out-of-plane displacement. The solid lines are analytical results (Westerweel 1993a, b); the symbols are obtained from Monte Carlo simulations (the error bar represents the uncertainty of the simulation result)

Random Errors are approximately independent of particle displacement

At displacement below <0.5 pixels random error decrease linearly

Random error is proportional to particle image diameter

$$\sigma_{\Delta X} \cong c d_\tau$$

Performance of Correlation Techniques
PIV Peak Locking (Bias Error)

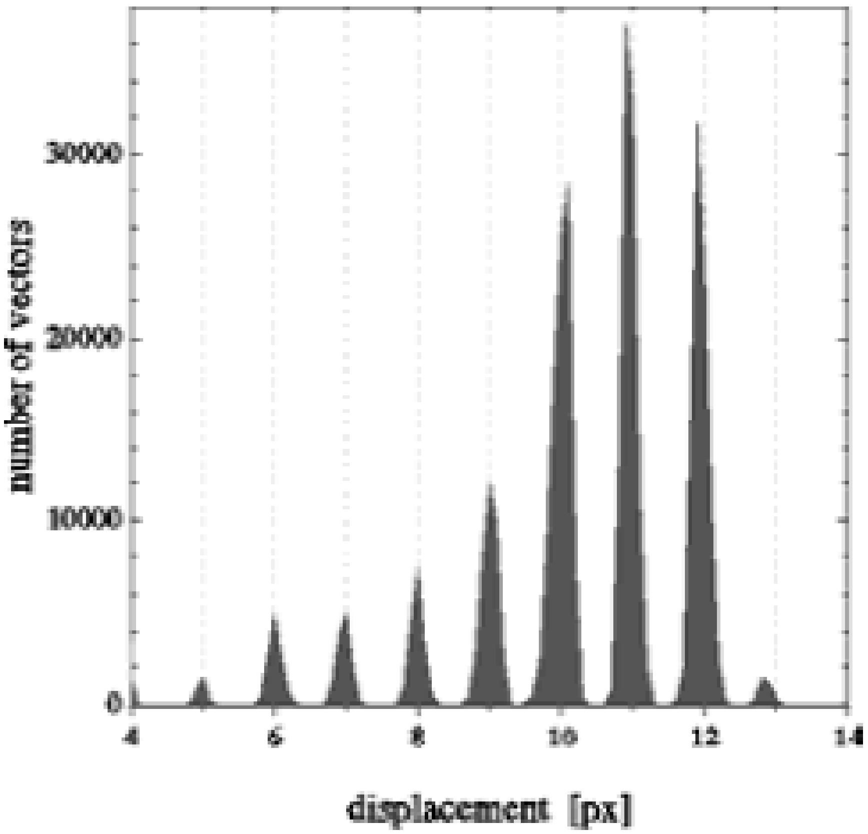

For particle size less than 2 pixel the displacement is biased towards integer values

The three point gaussian peak-fit is unsuited at these particle image diameter

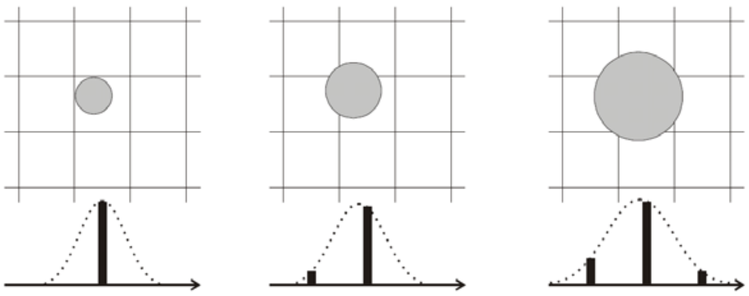

Performance of Correlation Techniques
PIV Bias Errors

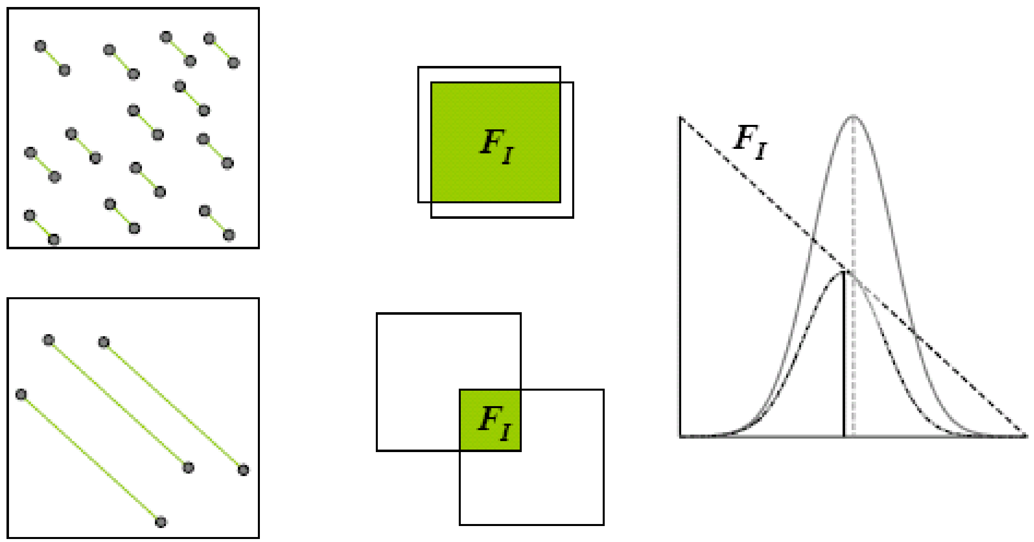

Estimated displacement are biased towards smaller value

- In plane loss of pare (large displacements gives less strong signal)
- Finite size of interrogation area

  Divide correlation with factor found from correlation of uniform signal

Performance of Correlation Techniques Optimization of Particle Image Diameter

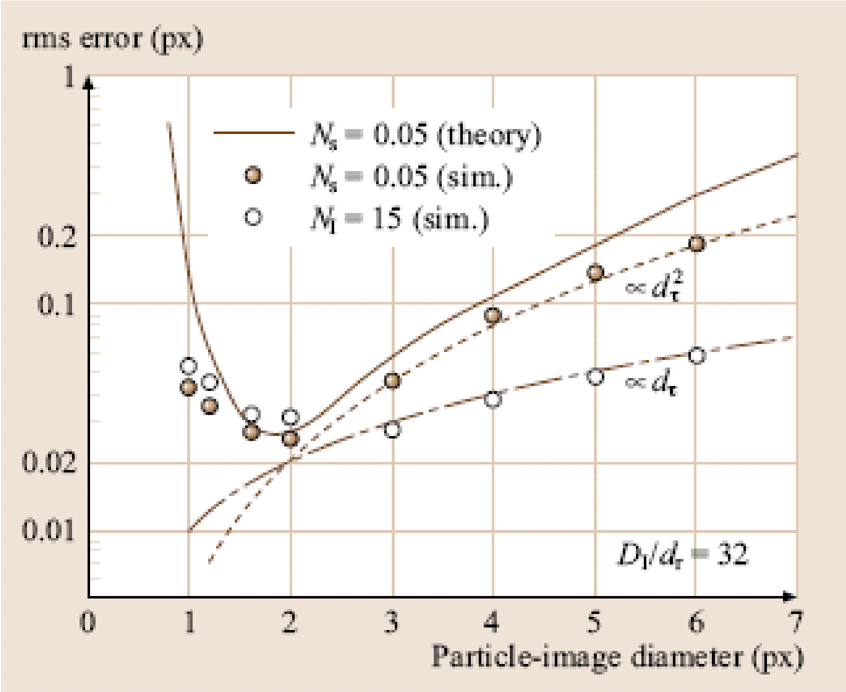

Fig. 5.112 The rms displacement error as a function of the particle image diameter (in pixel units) for 32×32 px interrogation windows and constant image density $N_I = 15$ (*open symbols*) and constant source density $N_s = 0.05$. The *solid line* represents a theoretical result, while the *dotted* and *dashed lines* represent scaling relations. (After *Westerweel* [5.433])

For cross-correlation technique and three point Gaussian peak-fit the optimum particle size is about 2-4 pixels

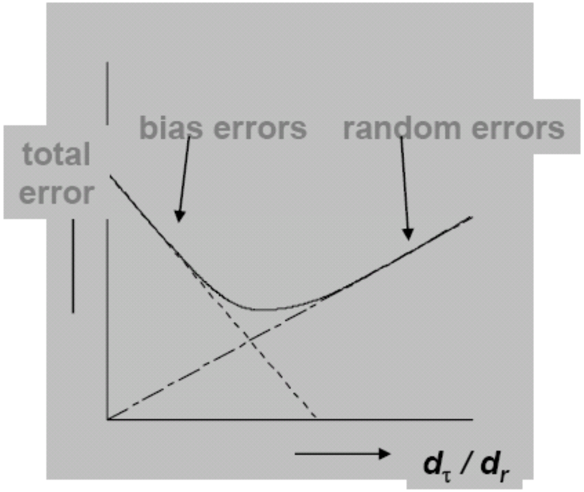

Performance of Correlation Techniques Interrogation Area Optimization

To minimize loss of pair and bias errors the size of Interrogation Area should fulfill the following conditions

Interrogation Area optimization

- Average number of particle images $$N = C\Delta z\pi\left[D_I/(2M)\right]^2 > 5 \div 10$$
  (C: number of particles per unit volume)
- Interrogation Area dimension: $$\left(u^2+v^2\right)^{1/2}\Delta t < D_I/4M$$
- Out-of-plane velocity component $$\mathrm{w}\Delta\mathrm{t} < \Delta\mathrm{z}/4$$
  (Δz: laser sheet thickness)
- Spatial gradients $$\left|\Delta\mathrm{u}\right|/\left|\mathrm{u}\right| < 0.2$$

In high *image density* (N_I) there are less problems than in low image density cases, where the experimental parameters need to be optimized.

Performance of Correlation Techniques Dynamic Velocity/Spatial Range

$$L_x / \Delta X_{\max} \sim L_x / D_I$$

dynamic spatial range $\quad \text{DSR} = \dfrac{\text{image format}}{\text{interrogation resolution}}$

dynamic velocity range $\quad \text{DVR} = \dfrac{\text{max. particle displacement}}{\text{displacement error}}$

$$\frac{\Delta X_{\max} - \Delta X_{\min}}{\Delta X_{\min}} = \frac{D_{\mathrm{I}}}{4\Delta X_{\min}} - 1 \,.$$

$$\Delta X_{\min} = 0.1 \text{ px}$$

system	format	DSR	DVR
standard video	768×494	50	140
large-format video	2029×1044	130	140
35 mm film	7000×4800	440	140
4”×5” film (Tmax)	25000×20000	1560	140
8”×10” film (TP)	160000×128000	10000	140

Advanced Digital Interrogation Technique

Recursive correlation processing allows to iteratively improve spatial resolution.

Recursive correlation processing uses first step correlation to obtain a mean displacement and direction. These data are used to define the centres of a search window for image pairing.

By offsetting the second interrogation windows the matched particle image increase (SNR of correlation peak increase).

Thus size of interrogation area can be reduced at each step without significantly affect the measurements uncertainty

Velocity maps of a swirling flow

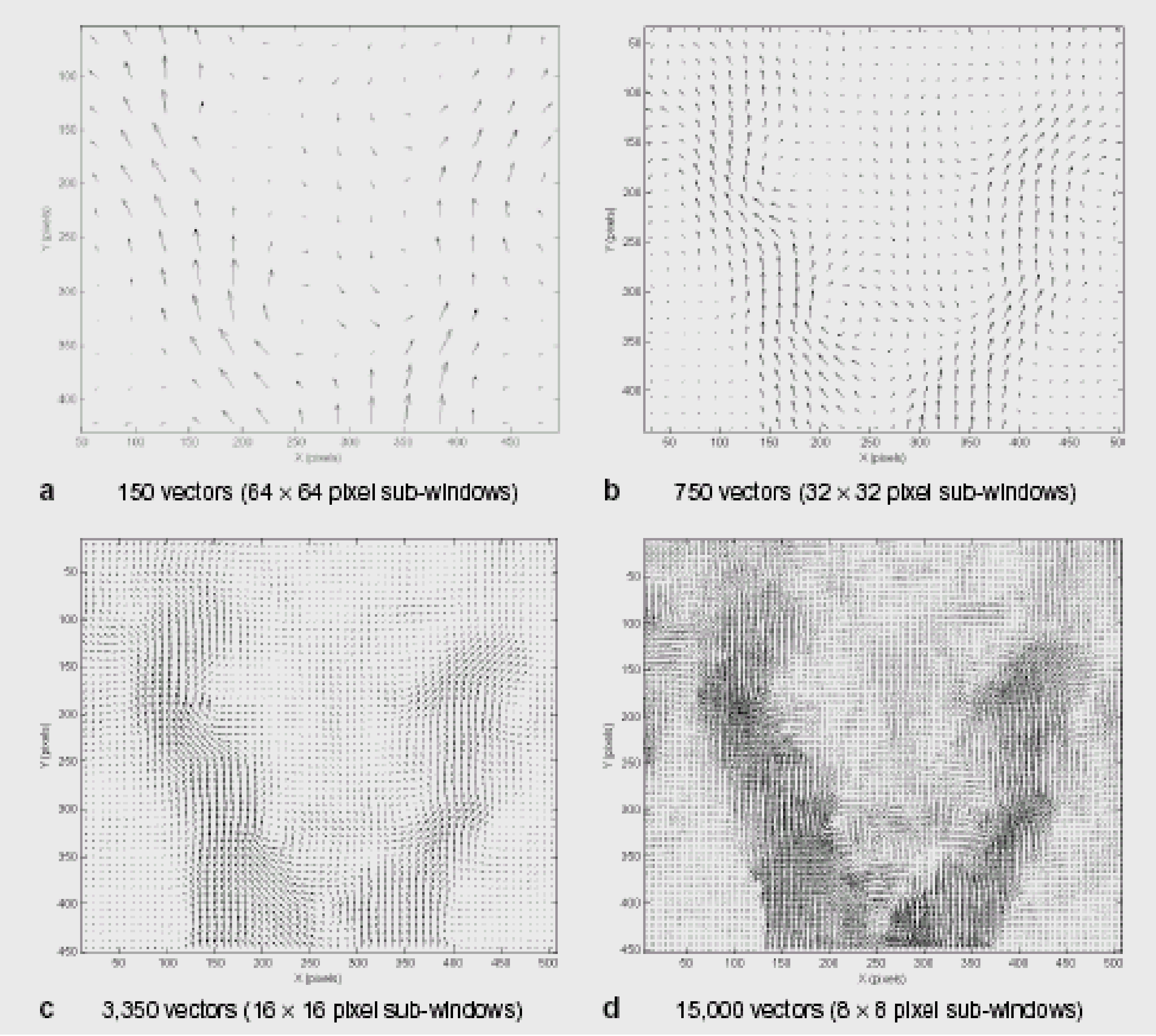

a 150 vectors (64 × 64 pixel sub-windows)

b 750 vectors (32 × 32 pixel sub-windows)

c 3,350 vectors (16 × 16 pixel sub-windows)

d 15,000 vectors (8 × 8 pixel sub-windows)

Advanced Digital Interrogation Technique

The pictures illustrate the possibility of processing PIV images to the limits of optical resolution, even when significant out of plane flow exists

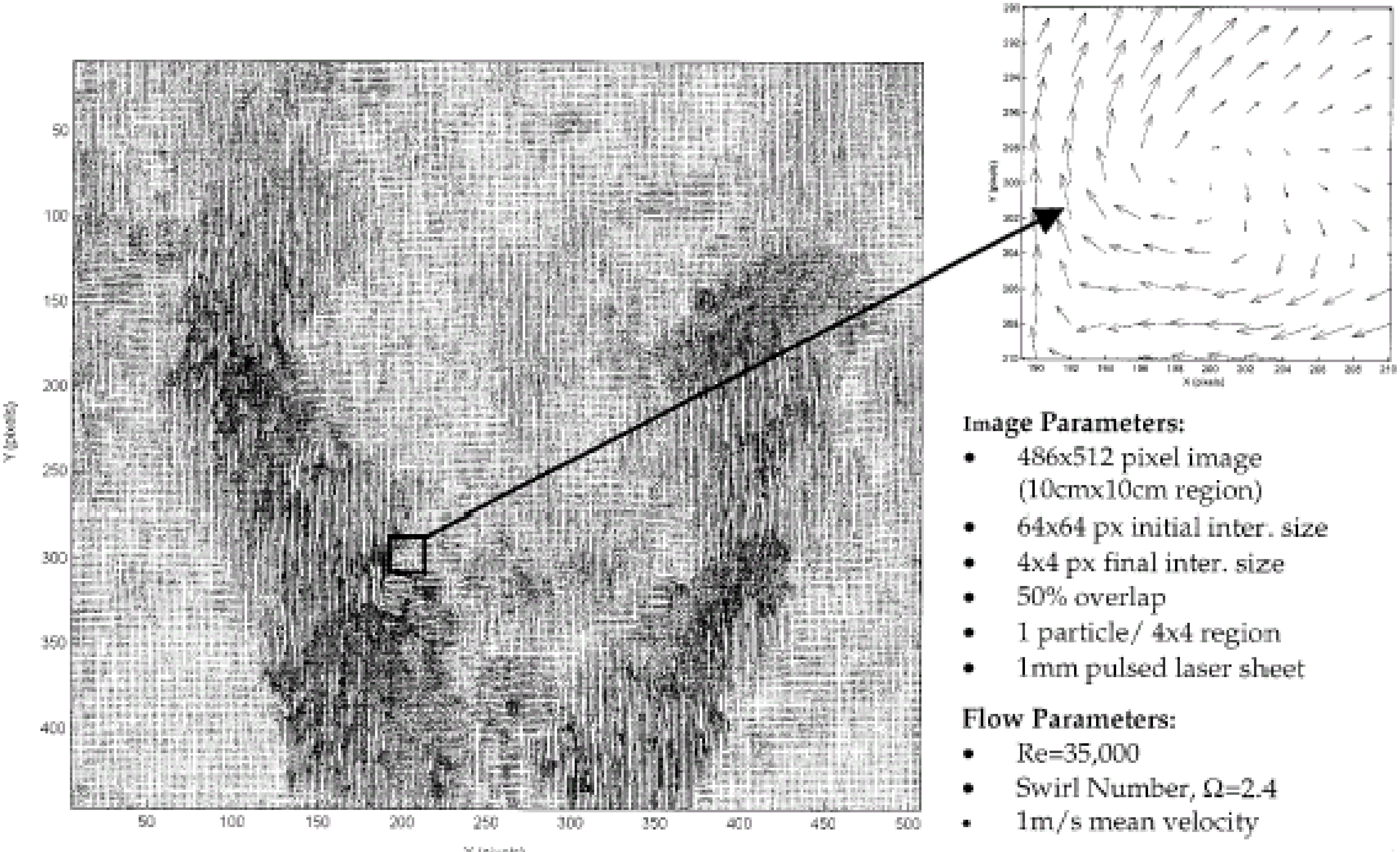

Developments of PIV
3-D PIV

Stereoscopic planar PIV measures the 3 dimensional velocity field in a plane

Sets of vector maps are recorded and calculated by cross correlation

The 3D vectors are reconstructed from projections of the two maps to the light sheet plane

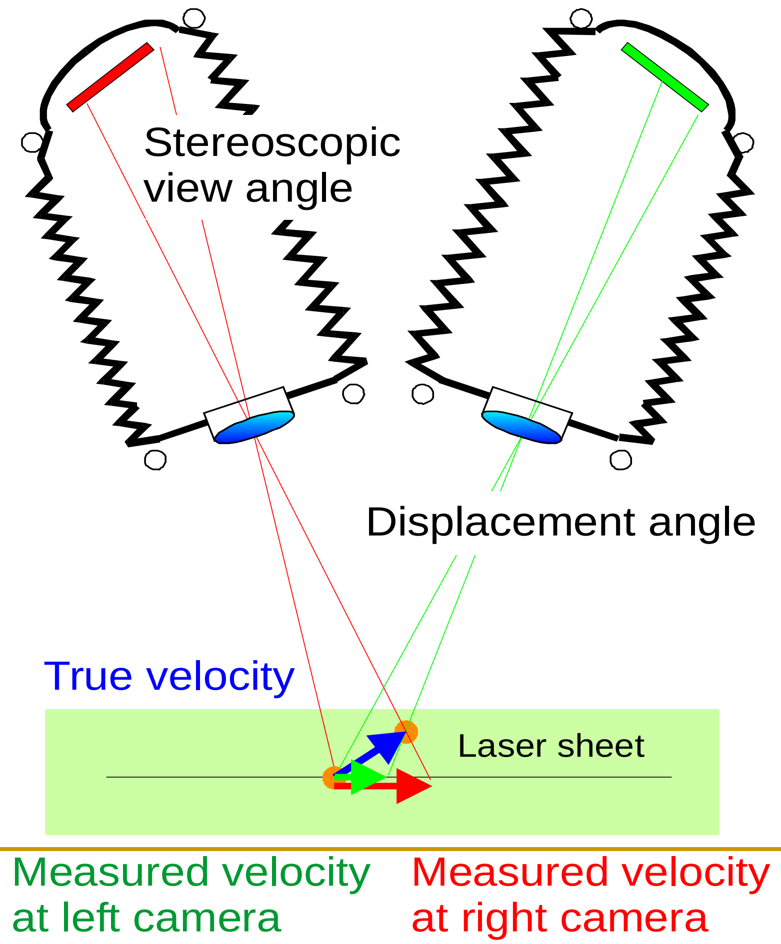

Developments of PIV
3-D PIV - Fundamentals of stereo vision

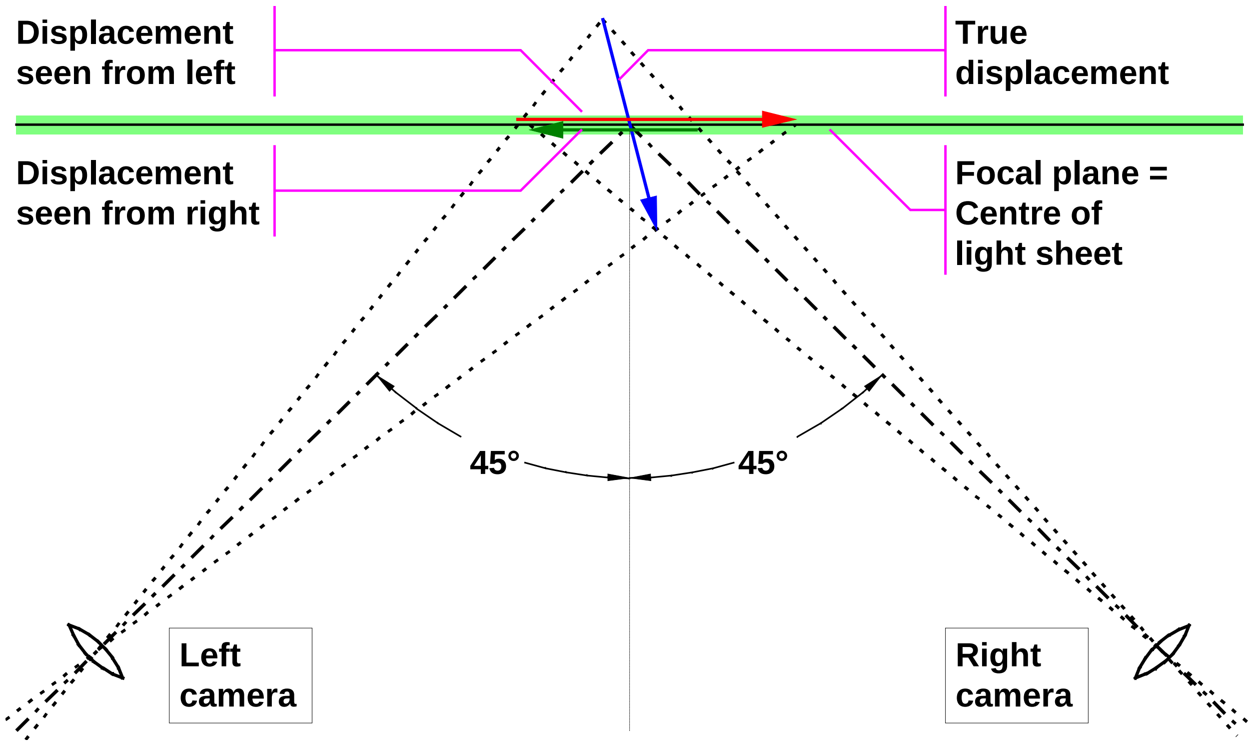

True 3D displacement is estimated from a pair of 2D displacements as seen from left and right camera respectively

Developments of PIV
3-D PIV

Focusing an off-axis camera requires tilting of the CCD-chip (Scheimpflug condition)

3D evaluation requires a numerical model, describing how objects in space are mapped onto the CCD-chip of each camera

Parameters for the numerical model are determined through camera calibration

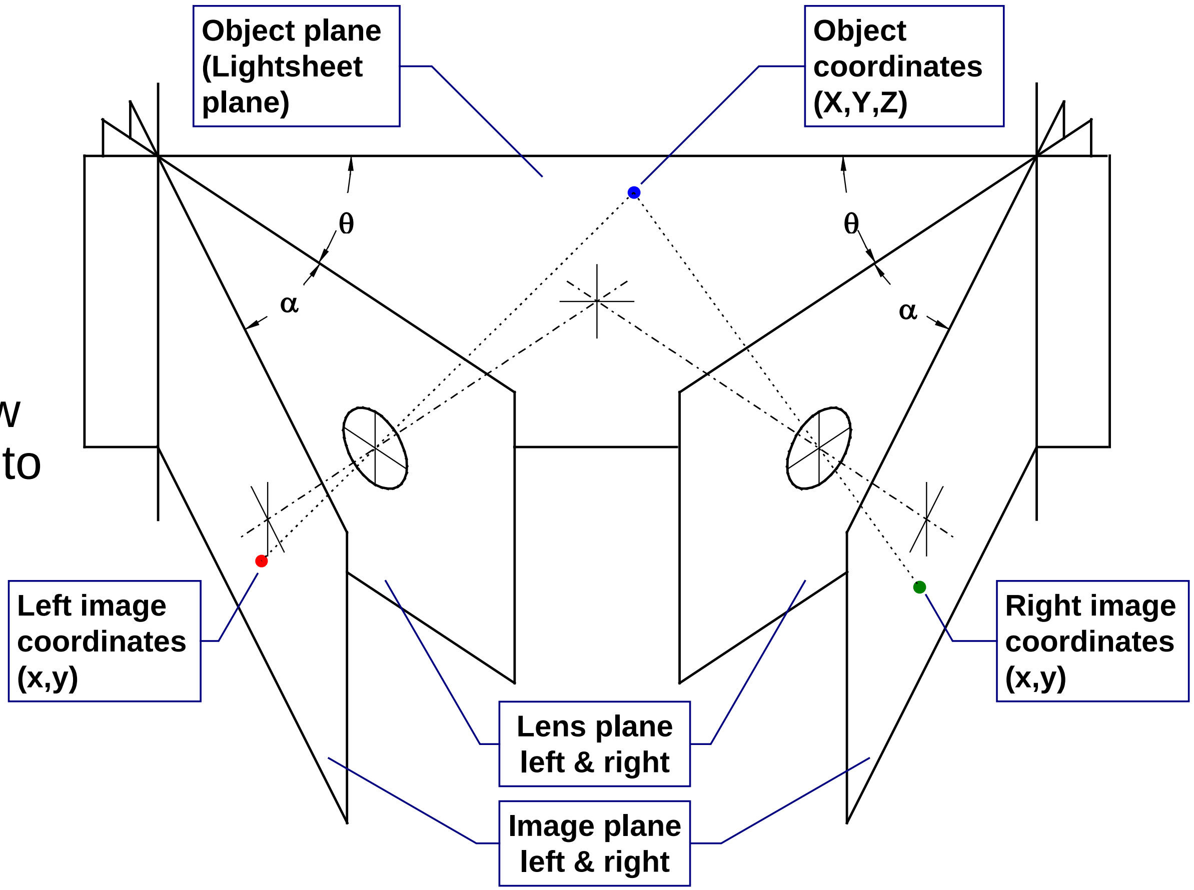

Developments of PIV
3-D PIV – Calibration

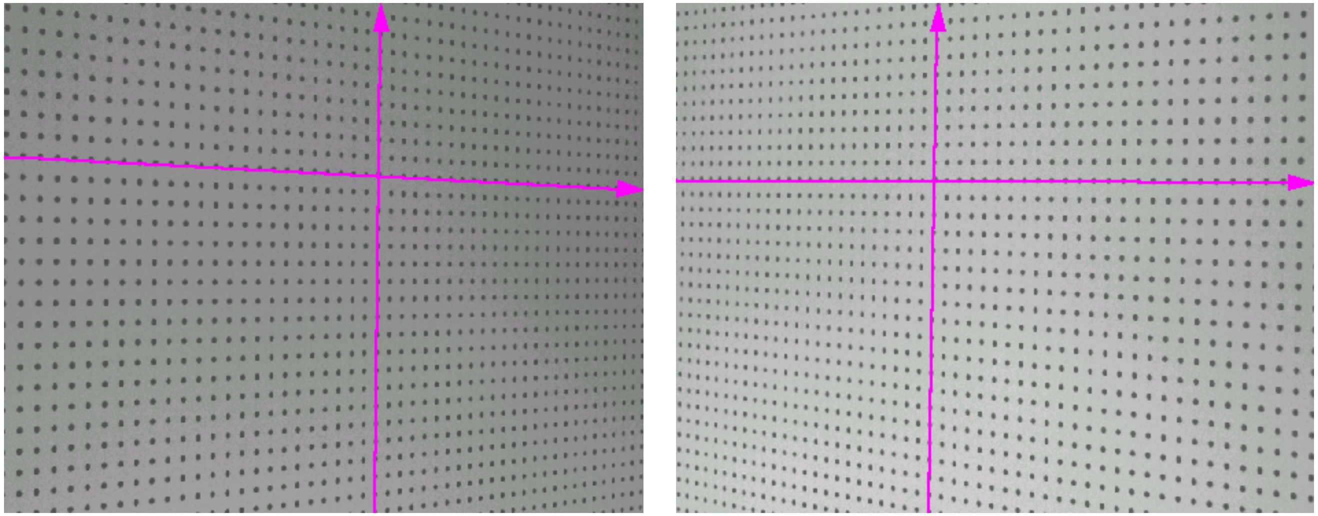

Images of a calibration target are recorded.

The target contains calibration markers in known positions.

Comparing known marker positions with corresponding marker positions on each camera image, model parameters are adjusted to give the best possible fit.

Developments of PIV
3-D PIV – Overlapping fields of view

3D evaluation is possible only within the area covered by both cameras.

Due to perspective distortion each camera covers a trapezoidal region of the light sheet.

Careful alignment is required to maximize the overlap area.

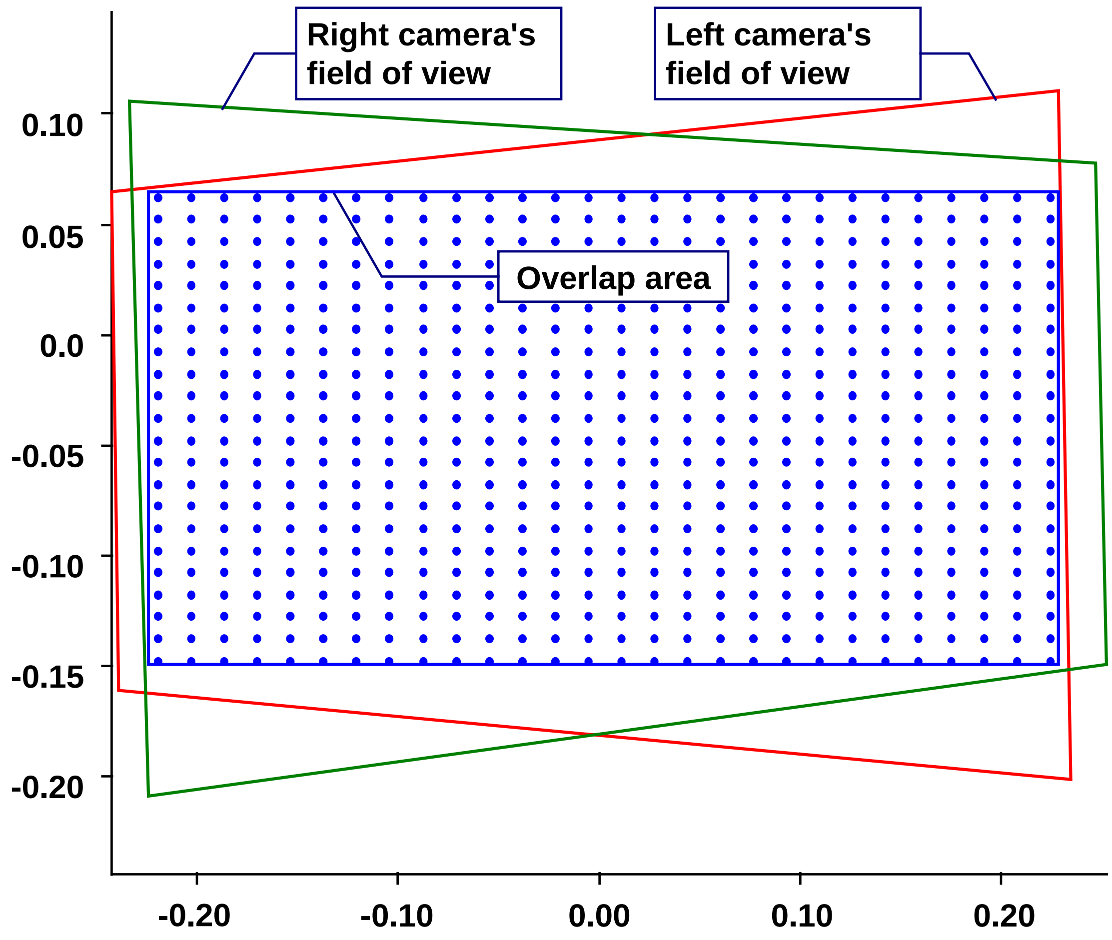

Developments of PIV
Time-Resolved PIV

Same principle as classical PIV

High frame rate with special laser and camera

Time resolved flow analysis

Hardware

Cw-diode pumped Nd:Yag laser

High-speed megapixel CMOS sensor

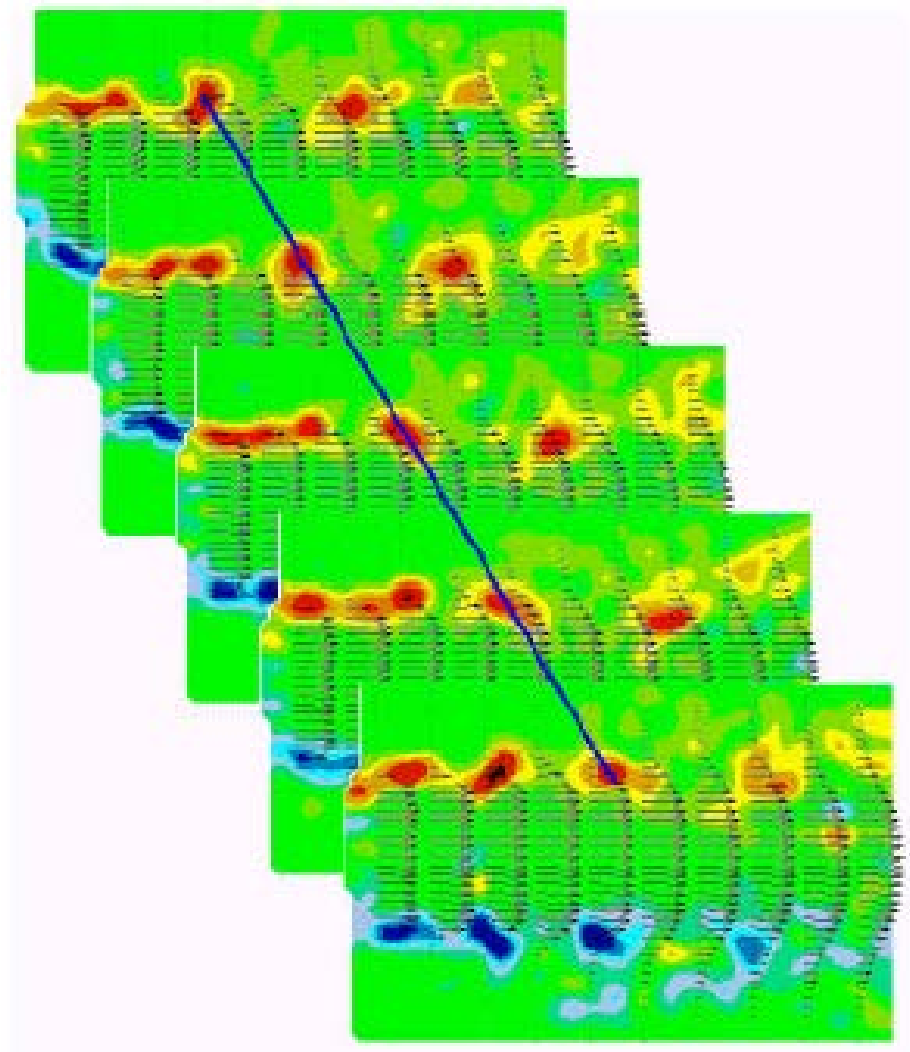

Developments of PIV
Micro-PIV

High Spatial resolution 100-10 μm

Particle smaller than laser light wavelength (Fluorescent seeding)

Volume illumination

Low particle density

Special correlation technique

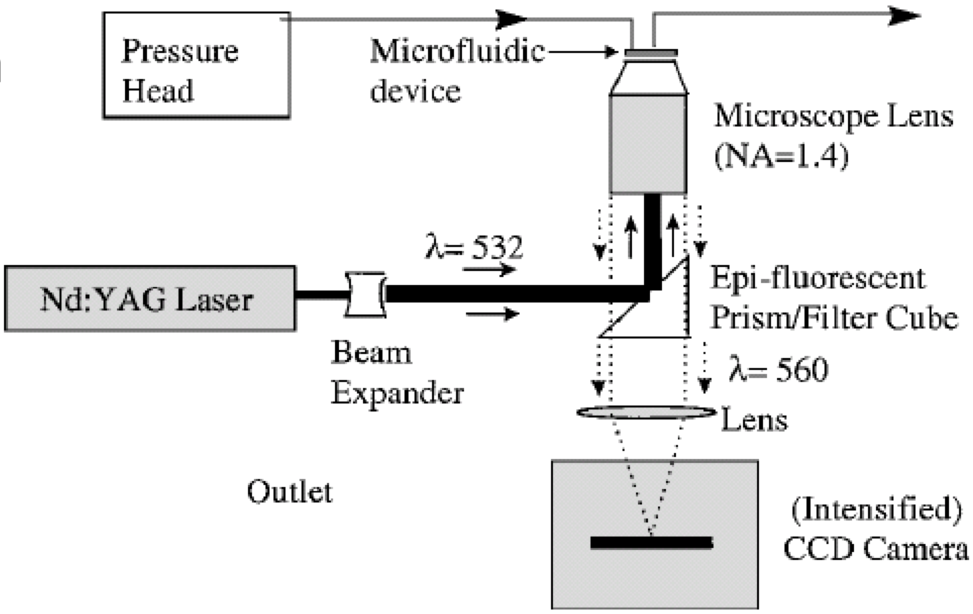

Fig. 1 Diagram of typical micro-PIV system.

PIV Applications

PIV technique has been applied to investigate a very broad range of technical and scientific problems.

- Gasdynamics, Fluidynamics, Combustion & Turbulence
  - Flow across shock waves
  - Turbomachinery (flow around turbine and compressor blades)
  - Laminar and turbulent flames
  - Swirl combustor (aerospace propulsion and stationary power systems)
  - Premixed and non premixed burners
- Aerospace
  - Flow inside rocket motors
  - Flow over wings
  - Wake of hovering rotor
- Car industry
  - Vehicle Aerodynamics
- Naval Hydrodynamics
  - Ship wakes
  - Propeller flows
  - Underwater vehicle hydrodynamics
- Bioengineering
  - Flow in artificial heart valves
  - Flow in lung
- Appliance
- …..

Examples of PIV Measurements

Measurements In a Swirling Air Flow

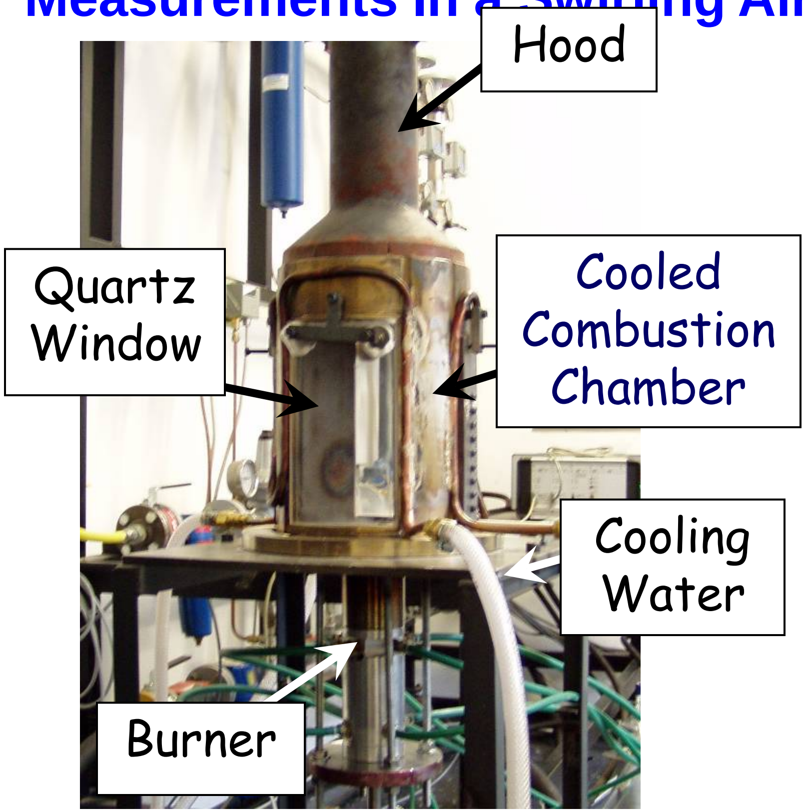

Burner geometry

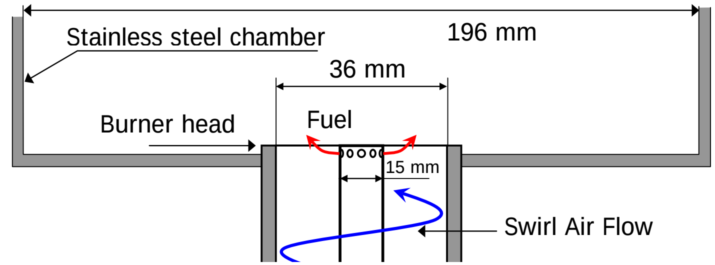

Burner - top view

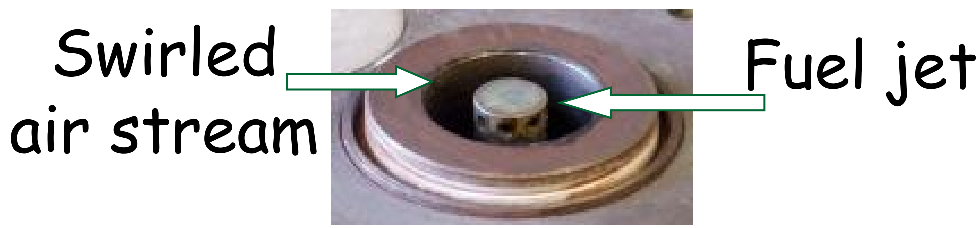

- Swirl generated by axial + tangential air injection
- Transverse fuel mixture injection
- Fuel injection below the burner exit (partial air/fuel mixing)

Examples of PIV Measurements

Measurements In a Swirling Air Flow

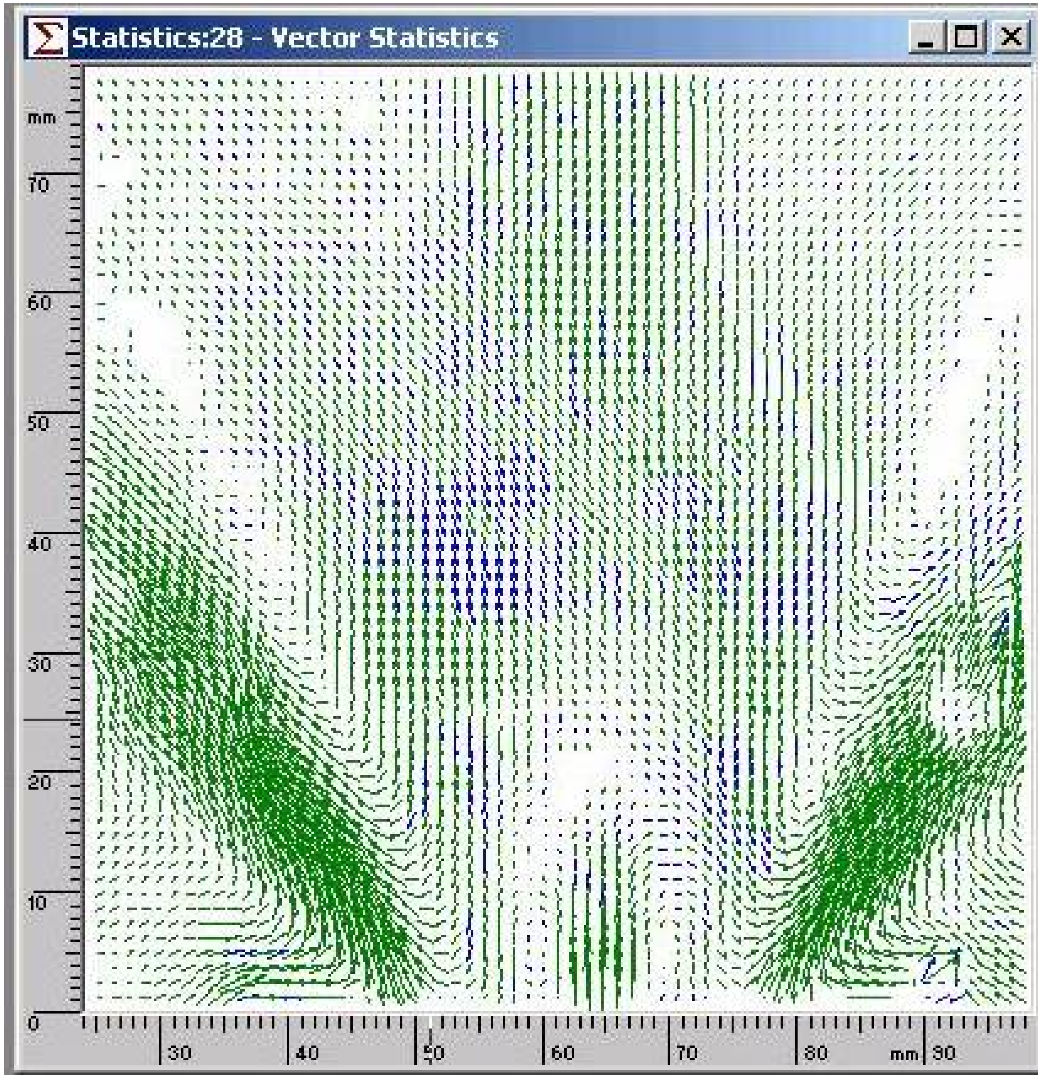

2-D mean velocity pattern in the axial section of a axi-symmetric swirling air flow.

Burner with two co-axial flows: inner jet and co-flow swirling air

A large toroidal recirculation region is generated in the central region.

Average over 200 double images

Green = positive velocities

Bleu= negative velocities

Examples of PIV Measurements

Measurements In a Swirling Air Flow

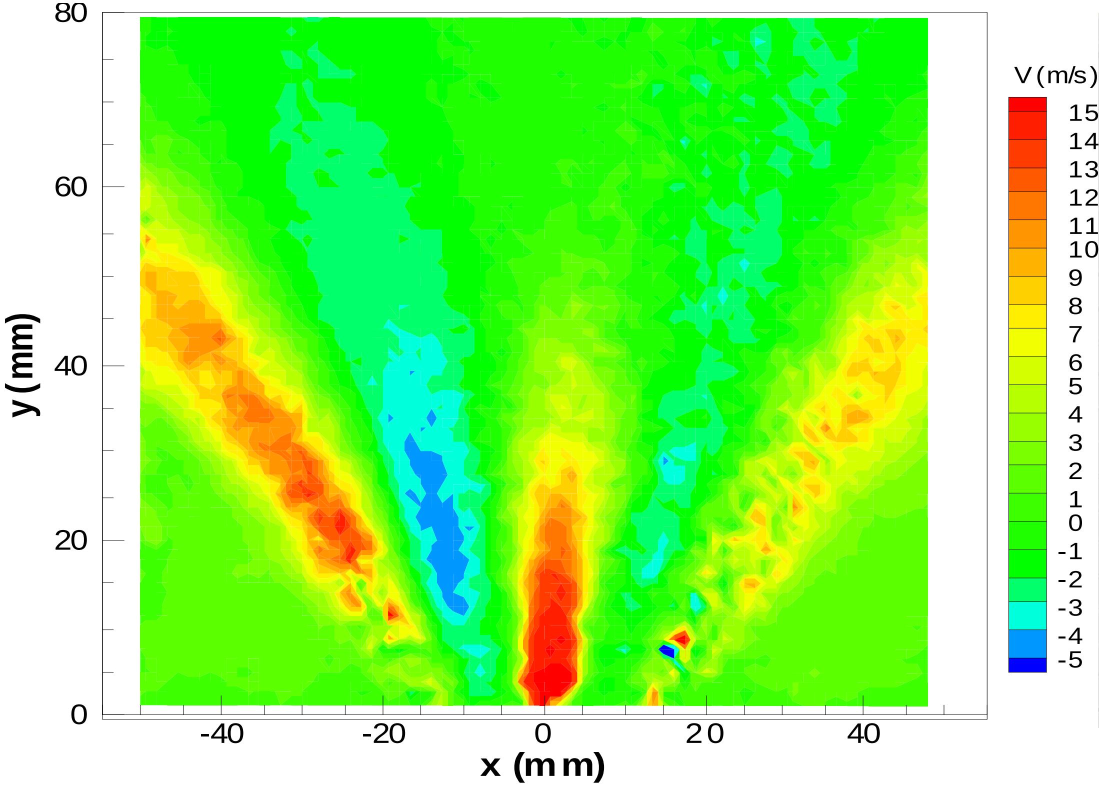

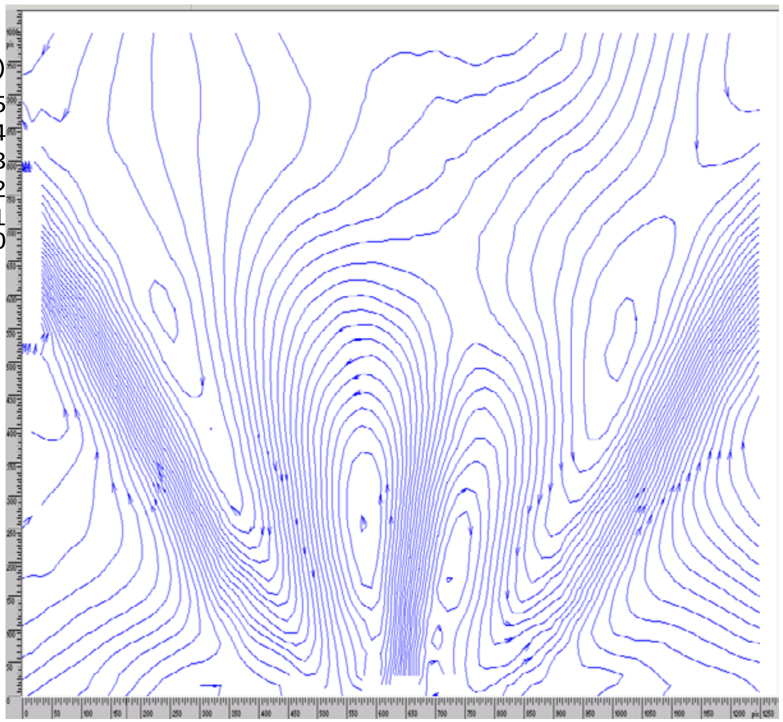

2D plot of the axial velocity component measured by PIV in a swirled natural gas flame (50% H_2) and streamlines

Examples of PIV Measurements

Average and instantaneous vortex core in a Swirling Air Flow

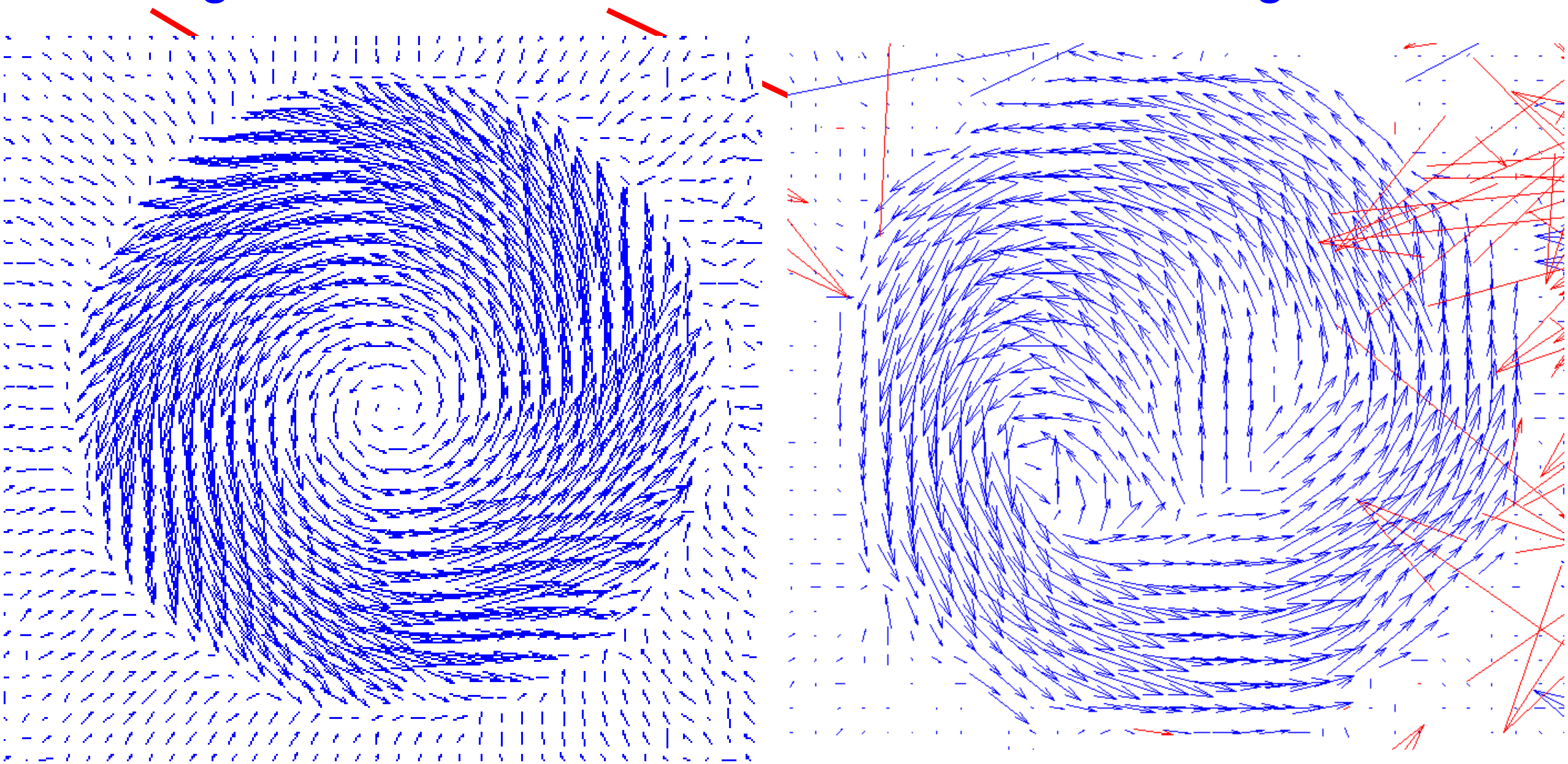

PIV measurements made in a swirling jet flow under PVC regime

Examples of PIV Measurements

Transonic Wind Tunnel

ONERA - Modane

Figure 1 : Profil d'aile dans la soufflerie transsonique S2 Modane.

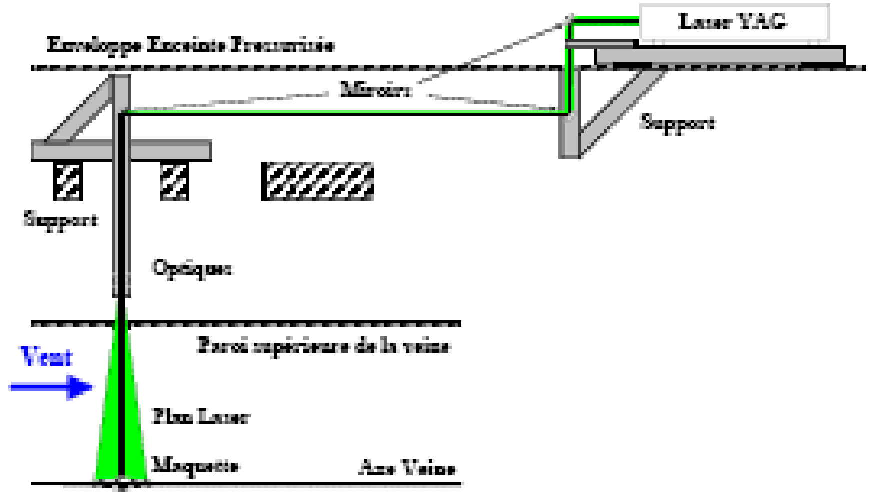

Figure 2 : Dispositif de génération de plan laser.

Examples of PIV Measurements

Transonic Wind Tunnel - ONERA - Modane

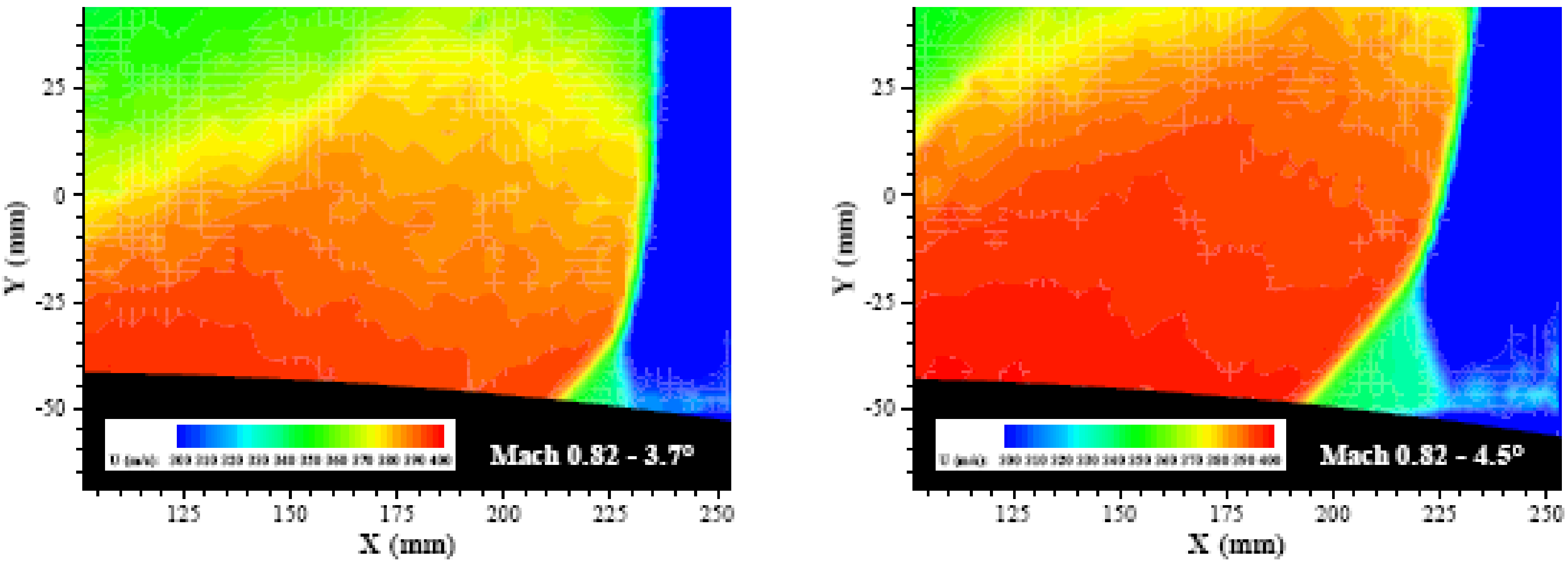

Figure 3 : Cartes de vitesses moyennes à Mach 0,82 et incidence 3.7° et 4.5°.

Mean velocity distribution in a lungitudinal plane of the wing extrados. PIV measurements show a shock on the wing extrados

Examples of PIV Measurements

3-D PIV in the wake of a hovering rotor

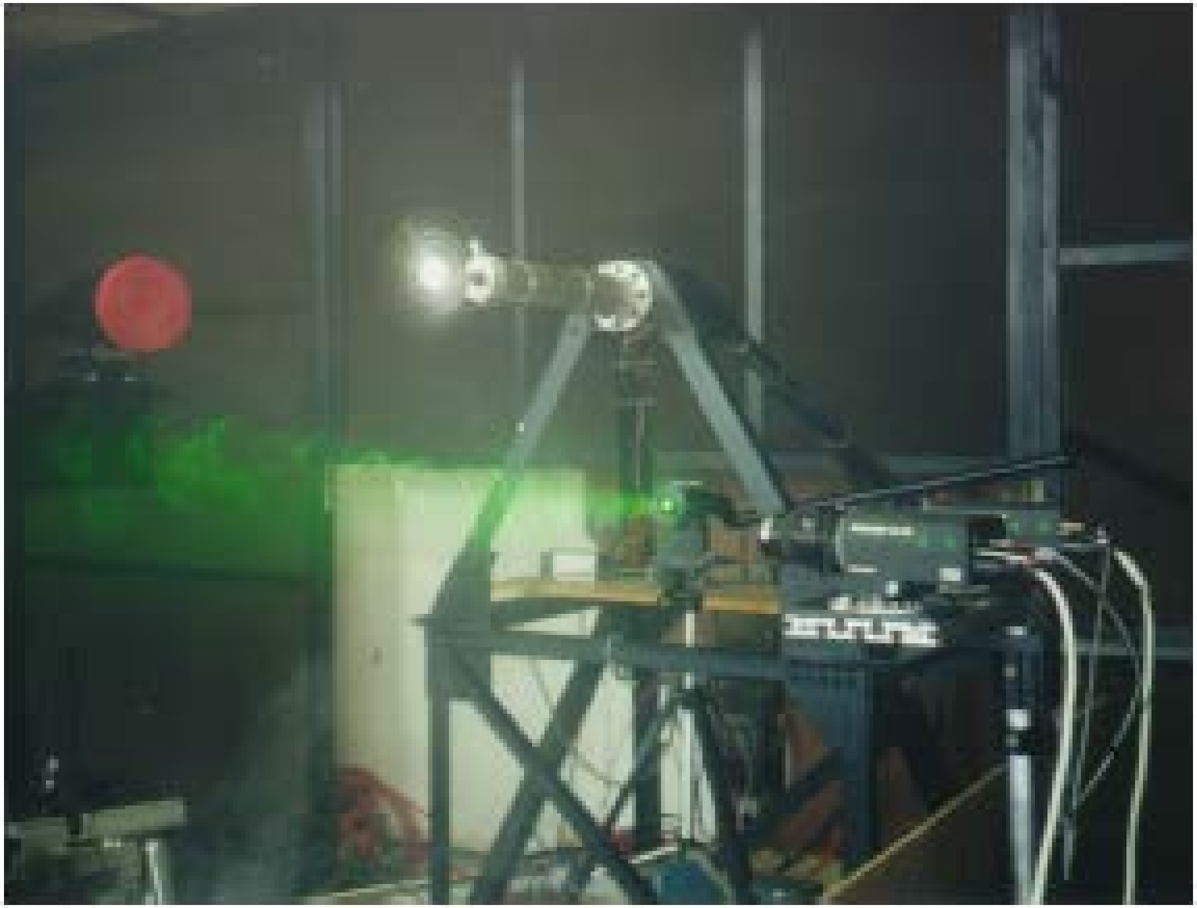

Figure 3: Rotor test stand and PIV apparatus.

Examples of PIV Measurements

3-D PIV in the wake of a hovering rotor

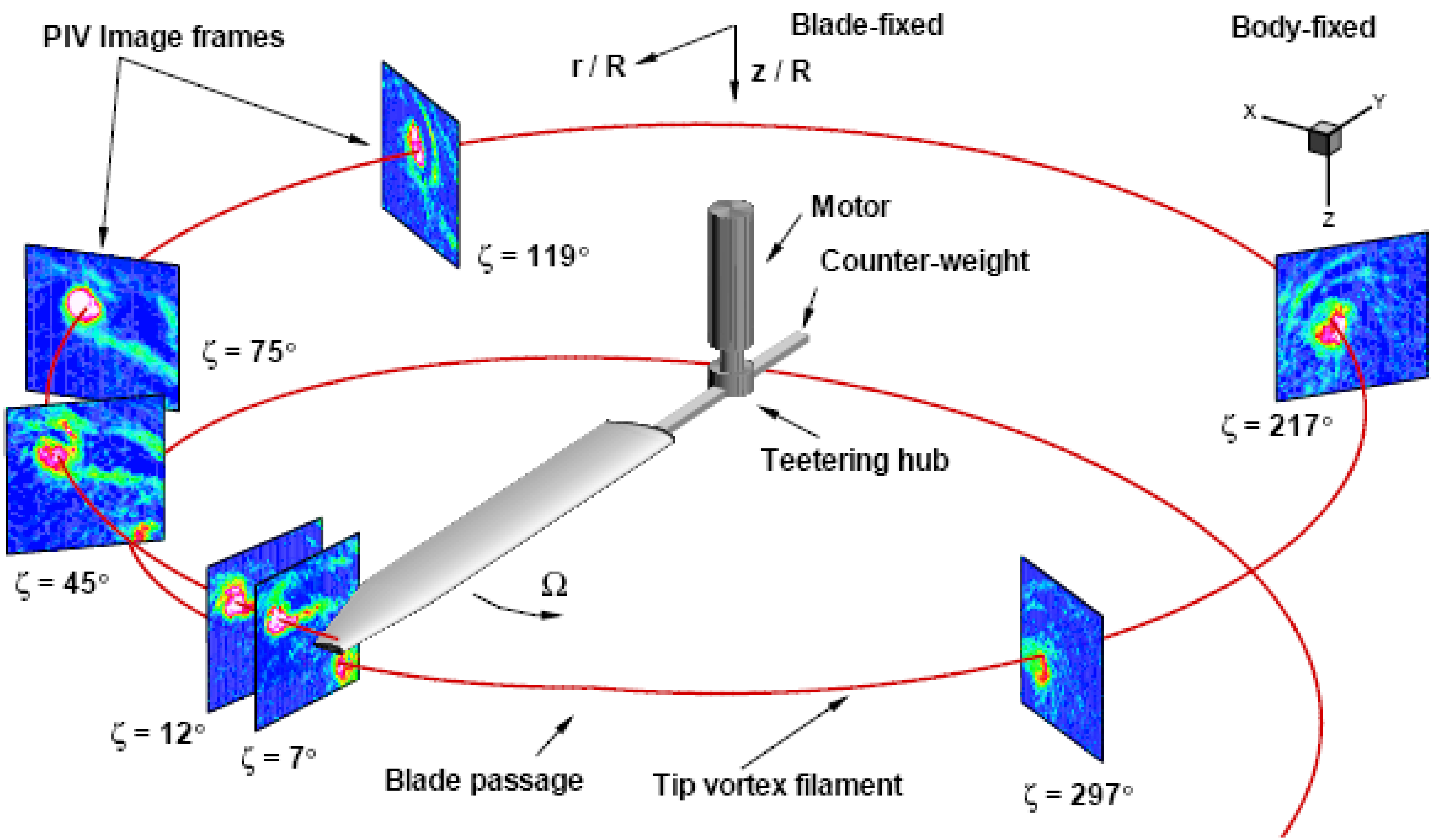

References

- Raffel, M. et al. *Particle Image Velocimetry. A Practical Guide,* Springer 2007
- *Handbook of Experimental Fluid Mechanics,* edited by Tropea C., Yarin A.L., Foss J.F., Springer 2007
- *Particle Image Velocimetry, New Developments and Recent Applications* Series: Topics in Applied Physics , Vol. 112, Schröder, Andreas; Willert, Christian E. (Eds.) 2008
- Adrian R.J. *Twenty years of particle image velocimetry,* Experiments in Fluids, 2005
- Grant I. *Particle image velocimetry: a review, IMechE 1997*